University of Alberta

The Effects of Fructose Feeding on the Quantal Catecholamine Release from Adrenal Chromaffin Cells

by

Michael Simpson

A thesis submitted to the Faculty of Graduate Studies and Research

in partial fulfillment of the requirements for the degree of

Master of Science

Centre for Neuroscience

Spring 2014

Edmonton, Alberta

Dedication:

To my father who supported me through all my endeavours

Abstract:

The fructose-fed rat is an animal model of metabolic syndrome, which includes the development of hypertension. In other animal models of hypertension, an increase in the amount catecholamine released from chromaffin cells was reported. Employing carbon fibre amperometry, I tested the hypothesis that fructose feeding causes an increase in the amount of catecholamine released from individual adrenal chromaffin cells. When I stimulated chromaffin cells from fructose-fed rats with a non-selective acetylcholine agonist, they secreted more catecholamine than cells from age-matched control rats, although the amplitude of the rise in intracellular Ca^{2+} (measured by fura-2) was not increased. Fructose feeding also increased the amount of catecholamine released from individual secretory granules. These changes in catecholamine release were not reproduced when the cells were stimulated by elevating the extracellular concentration of K^{+}. My findings suggest that fructose feeding may alter the expression or function of muscarinic acetylcholine receptors in chromaffin cells.

Acknowledgements:

The following people at the University of Alberta were instrumental to the completion of this thesis, there guidance has been invaluable: Dr. Fred Tse, Dr. Amy Tse, Lei Yan, Dr. Andy Lee, Su Su Liang and Weixiao (Iris) Zhao, Dr. Alexander Clanachan, Dr. Manoj Gandhi, Dr. Michael Zaugg, Dr. Glen Baker, Gail Rauw and Dr. Matthias Braun.

Table of Contents: Page(s)

Tables: **Page**

Chapter 3:

Chapter 4:

Figures: **Page**

Chapter 1:

Chapter 3:

Abbreviations List:

Ach	Acetylcholine
CCh	Carbachol
CFE	Carbon fibre electrode
DMSO	Dimethyl sulfoxide
Fura-2-AM	Fura-2-acetoxymethyl ester
HCSP	Highly calcium sensitive pool
HPLC	High performance liquid chromatography
IP_3	Inositol-trisphosphte
IRP	Immediately releasable pool
LDCG	Large dense core granule
mAChR	Muscarinic acetylcholine receptor
MMP-2	Matrix metallo proteinase
Munc18	Mammalian uncoordinated 18
nAChR	Nicotinic acetylcholine receptor
NO	Nitric oxide
PKC	Protein Kinase C
PNMT	Phenylethanolamine N-methyl transferase
Q	Quantal Size
RRP	Readily releasable pool
SNAP-25	Soluble NSF Attachment protein-25
SNARE	SNAP receptor
SRP	Slow releasable pool
VAMP-2	Vesicular associated membrane protein-2
VGCC	Voltage gated calcium channels
VMAT1	Vasicular monoamine transporter-1

Chapter 1 Introduction:

Anatomy and physiology of adrenal chromaffin cells

The adrenal gland is a secretory gland located just above the kidney and consists of two parts, the adrenal cortex and the adrenal medulla. The adrenal cortex is responsible for secreting corticosteroids into the blood stream, while the adrenal medulla is the endocrine effector for the stress response of the sympathetic nervous system (Kvetnansky et al., 2009). The chromaffin cells of the adrenal medulla secrete catecholamines, mainly adrenalin and noradrenalin, into the blood circulation (Kvetnansky et al., 2009). In response to acute stress, *e.g.* fight or flight response, acetylcholine (ACh) is released from the sympathetic nerve endings which innervate the adrenal medulla. In all mammalian species examined ACh activates nicotinic-acetylcholine receptors (nAChR) on the chromaffin cells which in turn cause the cell membrane of chromaffin cells to depolarize, which then activates their voltage-gated calcium channels (VGCC). The resulting influx of calcium into the chromaffin cells triggers fusion of large dense core granules (LDCGs) and release of their contents (Harkins & Fox, 1998;Taylor & Peers, 2000;Kvetnansky *et al.*, 2009;Borges *et al.*, 2010). Adrenal chromaffin cells also express muscarinic ACh (mACh) receptors, and in some species the activation of such receptors also contributes to the excitation and triggering of secretion (Guo *et al.*, 1996;Oomori *et al.*, 1998;Barbara *et al.*, 1998;Taylor & Peers, 2000). Adrenal chromaffin cells from most species studied can secrete both adrenalin and noradrenalin; however, approximately 80% of catecholamine released is adrenalin, and this ratio can vary based on the species and age of an animal (Lymperopoulos et al., 2007). When adrenalin is released from the adrenal medulla as a response to stress, an increase in the concentration of circulating catecholamine causes an increase in heart rate, blood pressure (by

causing constriction of the blood vessels) and blood glucose (so that more energy can be made available to muscles) (Kvetnansky *et al.*, 2009;Lymperopoulos *et al.*, 2007).

Synthesis, storage and secretion of catecholamine

To produce adrenalin in chromaffin cells first tyrosine hydroxylase (TH, which is the rate limiting enzyme of catecholamine production) converts tyrosine into L-3,4-dihydroxyphenylalanine (L-dopa) (Kvetnansky et al., 2009). Dopamine is synthesized from L-dopa by dopa decarboxylase, and then transported into granules by the vasicular monoamine transporter 1 (VMAT1) and converted into noradrenalin by dopamine-β-hydroxylase (Kvetnansky *et al.*, 2009;Becherer *et al.*, 2012;Colliver *et al.*, 2000). VMAT1 is a catecholamine H^+ antiporter, which exploits the low pH inside granules to drive the importation of catecholamine (Colliver *et al.*, 2000;Becherer *et al.*, 2012). Phenylethanolamine N-methyltransferase (PNMT) catalyzes the formation of adrenalin from noradrenalin; however since PNMT is cytosolic, noradrenalin must leak out of the granules to be converted, requiring adrenalin to be taken into the granules using VMAT1 (Kvetnansky *et al.*, 2009;Becherer *et al.*, 2012). Chromogranins are a component of the LDCG matrix and are responsible for packaging catecholamine into LDCGs (Borges *et al.*, 2010;Becherer *et al.*, 2012). For a mature LDCG to become part of the readily releasable pool, and thus undergo rapid exocytosis, it has be transported to the cell membrane and primed to release by forming a SNARE complex between the vesicular and plasma membrane (Becherer et al., 2012). The LDCGs are transported to the plasma membrane by the actin network (Neco *et al.*, 2004;Villanueva *et al.*, 2012). The SNARE complex is formed starting with the binding of synaptotagmin 1 on the LDCG to syntaxin 1 and SNAP-25 on the plasma membrane (Becherer et al., 2012). Vesicular-associated membrane protein 2 (VAMP2) is incorporated by mammalian uncoordinated 18 (Munc18) to create the

SNARE complex (Becherer et al., 2012). Synaptotagmin 1 is a calcium sensor which triggers exocytosis, through the SNARE complex, when there is an increase in the local calcium concentration (Becherer et al., 2012).

A modern method to detect quantal release of catecholamine

Using carbon fibre amperometry, catecholamine secretion from individual LDCGs can be detected at millisecond resolution and quantified (Albillos *et al.*, 1997;Gong *et al.*, 2003). Carbon fibre amperometry detects the release of oxidizable materials (such as catecholamines), which are secreted from individual LDCGs (Albillos *et al.*, 1997;Gong *et al.*, 2003). For example, as shown in Fig. 1A, when a chromaffin cell is stimulated with high $[K^+]$, multiple amperometric signals (or events) are recorded from the chromaffin cell over a five minute period. Because in amperometry each detected molecule of catecholamine is converted to the current carried by 2 electrons, the time integral of the amperometric current (*i.e.* the area under the entire trace) can be used to measure the total amount of catecholamine secreted. Furthermore, the amount of catecholamine released from the fusion of individual LDCGs of an individual spike-shaped amperometric event (the quantal size or Q) can be calculated from the time integral of that event (Fig. 1B) (Gong et al., 2003). If the individual amperometric spikes do not overlap in time this technique can determine the number of LDCGs and the kinetics of release from individual LDCGs that undergo exocytosis at the site of the carbon fibre after the cell is stimulated. The spike amplitude (the maximum current generated by the release of catecholamine), the 50-90% rise time (how quickly a granule undergoes full fusion), the half width (the time difference at 50% maximum amplitude and reflects the rate catecholamine is released from LDCGs) and the decay time constant τ (the depletion of catecholamine from the granule) can be examined (Fig. 1B). Some events have a pre-spike "foot" signal that results from

a small conductance fusion pore permitting the release of catecholamine before full fusion occurs (Albillos et al., 1997). For those signals that contain a pre-spike foot, the foot duration (how stable the fusion pore is) and foot amplitude (may reflect the size of the fusion pore) were examined (Fig. 1B).

A model of diet-induced hypertension: the fructose-fed rat

The fructose-fed rat is a model of diet-induced metabolic syndrome. The symptoms that fructose-fed rats display are high plasma insulin, high plasma triglyceride levels, insulin resistance and hypertension (Hwang *et al.*, 1987;Panchal & Brown, 2011;Zhou *et al.*, 2012). The fructose-fed rat model is ideal for studying the mechanisms involved in metabolic syndrome development because the weight of fructose-fed rats is not significantly different from age-matched control rats, so there are no complications caused by having an obese rat (Dai & McNeill, 1995;Tran *et al.*, 2009). It is important to understand how fructose contributes to the development of metabolic syndrome symptoms since the incidence of metabolic syndrome and the use of fructose in our diets have increased significantly over the last 20 years (Panchal & Brown, 2011).

How does fructose feeding lead to the development of hypertension?

The focus of this project is to observe whether the development of hypertension in fructose-fed rats involves an increase in catecholamine secretion from individual adrenal chromaffin cells. Previous research has explored some possible causes of hypertension in fructose-fed rats so that strategies of treatment can be developed. Endothelial dysfunction has been implicated in the development of hypertension. Most recently Nagareddy *et. al.* (2012) showed that the inhibition of matrix metalloproteinase-2 (MMP-2) in fructose-fed rats could

stop the development of hypertension (Nagareddy et al., 2012). This yields the possibility that an increase in MMP-2 activity will reduce eNOS activity through proteolytic cleavage and thus decreases nitric oxide (NO), leading to more vasoconstriction (Tran *et al.*, 2009;Nagareddy *et al.*, 2012). The sympathetic nervous system has also been shown to play a role in the development of hypertension in the fructose-fed rats (Tran et al., 2009). Treatment of fructose-fed rats with clonidine (a central nervous system α_2-agonist that inhibits the sympathetic nervous system) prevented hypertension from developing, but failed to prevent an increase in plasma insulin and triglyceride levels (Hwang *et al.*, 1987;Tran *et al.*, 2009). Verma *et. al.* (1999) showed that when fructose-fed rats underwent a sympathectomy (*i.e.* the removal of the adrenal medulla) and were administered 6-hydroxydopamine (an isomer of noradrenalin which can selectively abate adrenergic sympathetic neuron signalling) they did not develop hypertension or hyperinsulinemia (Kostrzewa & Jacobowitz, 1974;Verma *et al.*, 1999). A later study by Hsien and Huang (2001) examined the role of the peripheral sympathetic nervous system by injecting neonatal rats with guanethidine (a false transmitter that inhibits the peripheral sympathetic nervous system by acting as a substrate of the noradrenalin transporter and hence replaces noradrenalin in the vesicles of post-ganglionic adrenergic neurons but leaves the central nervous system and adrenal medullas intact), and observed a reduction in hypertension and plasma triglyceride levels, but not a full prevention of either of these symptoms or any change in the plasma insulin and glucose levels (Hsien & Huang, 2001). This study suggests that the peripheral sympathetic nervous system is involved in the development of hypertension, but there are other factors that contribute to the development of hypertension (Hsien & Huang, 2001;Tran *et al.*, 2009). In addition, Kamide *et. al.* (2002) found that urinary output of both adrenalin and noradrenalin were significantly increased in the fructose-fed rats over control rats, which suggests that the secretion

of such molecules from endocrine sources is elevated (Kamide et al., 2002). If the adrenal medulla is involved in the development of hypertension there could be two ways in which the adrenal chromaffin cells have higher outputs of catecholamine. They could receive more stimulation from the central sympathetic nervous system and/or they could have an increase in the quantal secretion from individual chromaffin cells even when their excitation was unchanged.

An example of increased quantal secretion from adrenal chromaffin cells contributing to the development of hypertension can be found in the spontaneously hypertensive rat (Miranda-Ferreira et al., 2008). The spontaneously hypertensive rat is a Wistar rat which has been selectively bred to develop hypertension later in life (Miranda-Ferreira *et al.*, 2008;Segura-Chama *et al.*, 2010). When a bilateral adrenalectomy was performed before the development of hypertension, no hypertension was detected later (Segura-Chama et al., 2010). Chromaffin cells isolated from the spontaneously hypertensive rat not only release a larger total amount of catecholamine with the same stimulus, but individual amperometric signals have a larger quantal size (Miranda-Ferreira et al., 2008). This indicates that a larger amount of catecholamine secretion can be linked to increased catecholamine secretion from the adrenal gland.

A recent paper by Kinote *et al.* (2012) shows that rats which received intraperitoneal injections of fructose, three times a day for five days, had elevated levels of corticosterone (Kinote et al., 2012). Application of a glucocorticoid agonist leads to more cellular catecholamine in chromaffin cells and may increase the mean amount of catecholamine released from individual LDCGs through up-regulation of tyrosine hydroxylase (the rate limiting enzyme in catecholamine production) (Elhamdani *et al.*, 2000;Xu *et al.*, 2005). In this thesis, I examined the release of catecholamine from individual adrenal chromaffin cells to determine if there is an

increase in secretion similar to what is found in the spontaneously hypertensive rat. I also examined the total catecholamine content to determine if the increase in corticosterone levels found by Kinote *et. al.* (2012) have an effect on the total catecholamine content of the adrenal chromaffin cells.

Figures:

Figure 1:

A)

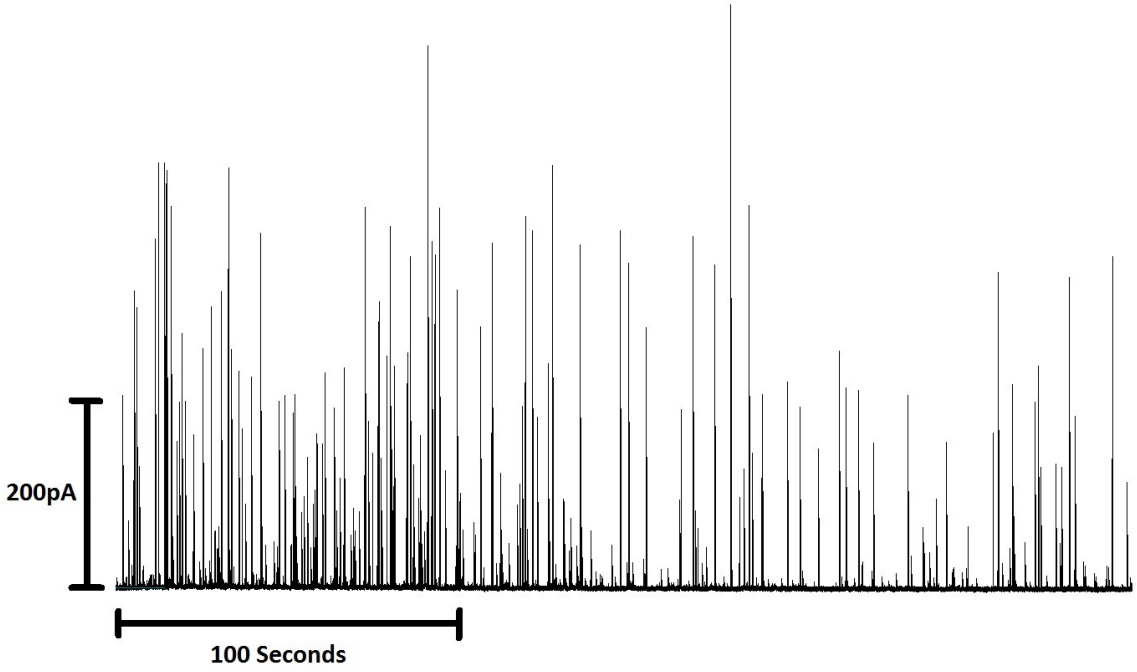

B)

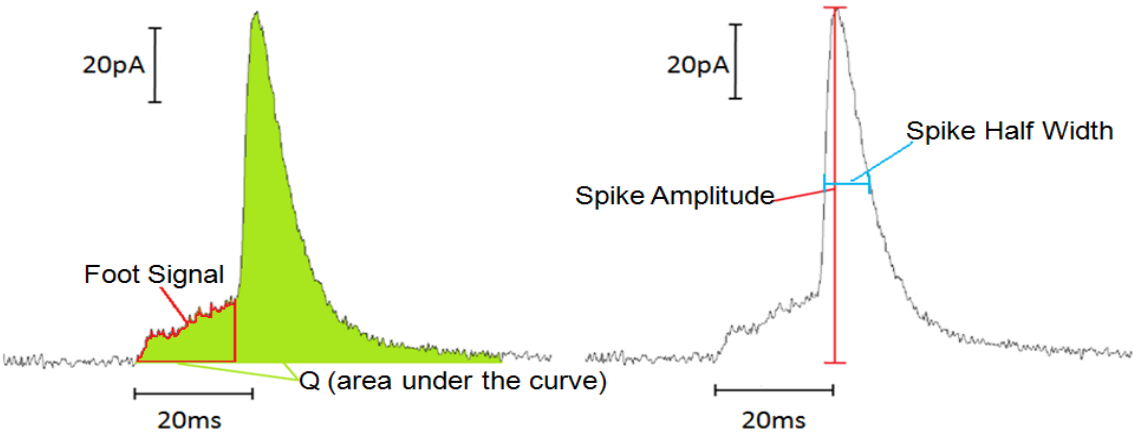

Figure 1A is an example of a five minute recording of a contol cell stimulated with 50mM KCl. Figure 1B shows a typical amperometric event which represents the release of one LDCG. Figure 1B also depictes the various kinetic parameters which are measured from a event.

Reference List:

Albillos A, Dernick G, Horstmann H, Almers W, Alvarez de TG, & Lindau M (1997). The exocytotic event in chromaffin cells revealed by patch amperometry. *Nature* **389**, 509-512.

Barbara JG, Lemos VS, & Takeda K (1998). Pre- and post-synaptic muscarinic receptors in thin slices of rat adrenal gland. *Eur J Neurosci* **10**, 3535-3545.

Becherer U, Medart MR, Schirra C, Krause E, Stevens D, & Rettig J (2012). Regulated exocytosis in chromaffin cells and cytotoxic T lymphocytes: how similar are they? *Cell Calcium* **52**, 303-312.

Borges R, Diaz-Vera J, Dominguez N, Arnau MR, & Machado JD (2010). Chromogranins as regulators of exocytosis. *J Neurochem* **114**, 335-343.

Colliver TL, Pyott SJ, Achalabun M, & Ewing AG (2000). VMAT-Mediated changes in quantal size and vesicular volume. *J Neurosci* **20**, 5276-5282.

Dai S & McNeill JH (1995). Fructose-induced hypertension in rats is concentration- and duration-dependent. *J Pharmacol Toxicol Methods* **33**, 101-107.

Elhamdani A, Brown ME, Artalejo CR, & Palfrey HC (2000). Enhancement of the dense-core vesicle secretory cycle by glucocorticoid differentiation of PC12 cells: characteristics of rapid exocytosis and endocytosis. *J Neurosci* **20**, 2495-2503.

Gong LW, Hafez I, Alvarez de TG, & Lindau M (2003). Secretory vesicles membrane area is regulated in tandem with quantal size in chromaffin cells. *J Neurosci* **23**, 7917-7921.

Guo X, Przywara DA, Wakade TD, & Wakade AR (1996). Exocytosis coupled to mobilization of intracellular calcium by muscarine and caffeine in rat chromaffin cells. *J Neurochem* **67**, 155-162.

Harkins AB & Fox AP (1998). Activation of nicotinic acetylcholine receptors augments calcium channel-mediated exocytosis in rat pheochromocytoma (PC12) cells. *J Gen Physiol* **111**, 257-269.

Hsien PS & Huang WC. Neonatal chemical sympathectomy attenuates fructose-induced hypertriglyceridemia and hypertension in rats. *Chinese Physiol* 44, 25-31. 2001.

Hwang IS, Ho H, Hoffman BB, & Reaven GM (1987). Fructose-induced insulin resistance and hypertension in rats. *Hypertension* **10**, 512-516.

Kamide K, Rakugi H, Higaki J, Okamura A, Nagai M, Moriguchi K, Ohishi M, Satoh N, Tuck ML, & Ogihara T (2002). The renin-angiotensin and adrenergic nervous system in cardiac hypertrophy in fructose-fed rats. *Am J Hypertens* **15**, 66-71.

Kinote A, Faria JA, Roman EA, Solon C, Razolli DS, Ignacio-Souza LM, Sollon CS, Nascimento LF, de Araujo TM, Barbosa AP, Lellis-Santos C, Velloso LA, Bordin S, & Anhe GF (2012). Fructose-induced hypothalamic AMPK activation stimulates hepatic PEPCK and gluconeogenesis due to increased corticosterone levels. *Endocrinology* **153**, 3633-3645.

Kostrzewa RM & Jacobowitz DM (1974). Pharmacological actions of 6-hydroxydopamine. *Pharmacol Rev* **26**, 199-288.

Kvetnansky R, Sabban EL, & Palkovits M (2009). Catecholaminergic systems in stress: structural and molecular genetic approaches. *Physiol Rev* **89**, 535-606.

Lymperopoulos A, Rengo G, & Koch WJ (2007). Adrenal adrenoceptors in heart failure: fine-tuning cardiac stimulation. *Trends Mol Med* **13**, 503-511.

Miranda-Ferreira R, de PR, de Diego AM, Caricati-Neto A, Gandia L, Jurkiewicz A, & Garcia AG (2008). Single-vesicle catecholamine release has greater quantal content and faster kinetics in chromaffin cells from hypertensive, as compared with normotensive, rats. *J Pharmacol Exp Ther* **324**, 685-693.

Nagareddy PR, Rajput PS, Vasudevan H, McClure B, Kumar U, Macleod KM, & McNeill JH (2012). Inhibition of matrix metalloproteinase-2 improves endothelial function and prevents hypertension in insulin-resistant rats. *Br J Pharmacol* **165**, 705-715.

Neco P, Giner D, Viniegra S, Borges R, Villarroel A, & Gutierrez LM (2004). New roles of myosin II during vesicle transport and fusion in chromaffin cells. *J Biol Chem* **279**, 27450-27457.

Oomori Y, Habara Y, & Kanno T (1998). Muscarinic and nicotinic receptor-mediated Ca^{2+} dynamics in rat adrenal chromaffin cells during development. *Cell Tissue Res* **294**, 109-123.

Panchal SK & Brown L (2011). Rodent models for metabolic syndrome research. *J Biomed Biotechnol* **2011**, 351982.

Segura-Chama P, Hernandez A, Jimenez-Perez N, Alejandre-Garcia T, Rivera-Cerecedo CV, Hernandez-Guijo J, & Hernandez-Cruz A (2010). Comparison of Ca^{2+} currents of chromaffin cells from normotensive Wistar Kyoto and spontaneously hypertensive rats. *Cell Mol Neurobiol* **30**, 1243-1250.

Taylor SC & Peers C (2000). Three distinct Ca(2+) influx pathways couple acetylcholine receptor activation to catecholamine secretion from PC12 cells. *J Neurochem* **75**, 1583-1589.

Tran LT, Yuen VG, & McNeill JH (2009). The fructose-fed rat: a review on the mechanisms of fructose-induced insulin resistance and hypertension. *Mol Cell Biochem* **332**, 145-159.

Verma S, Bhanot S, & McNeill JH (1999). Sympathectomy prevents fructose-induced hyperinsulinemia and hypertension. *Eur J Pharmacol* **373**, R1-R4.

Villanueva J, Torres V, Torregrosa-Hetland CJ, Garcia-Martinez V, Lopez-Font I, Viniegra S, & Gutierrez LM (2012). F-actin-myosin II inhibitors affect chromaffin granule plasma membrane distance and fusion kinetics by retraction of the cytoskeletal cortex. *J Mol Neurosci* **48**, 328-338.

Xu J, Tang KS, Lu VB, Weerasinghe CP, Tse A, & Tse FW (2005). Maintenance of quantal size and immediately releasable granules in rat chromaffin cells by glucocorticoid. *Am J Physiol Cell Physiol* **289**, C1122-C1133.

Zhou K, Kumar U, Yuen VG, & McNeill JH (2012). The effects of phentolamine on fructose-fed rats. *Can J Physiol Pharmacol* **90**, 1075-1085.

Chapter 2 Materials and Methods:

Cell dissociation:

Cells were made according to procedures previously described in Xu and Tse (1999) and Tang *et al.* (2005). Male Sprague-Dawley rats (300-400g) were euthanized in accordance with the standards of the Canadian Council on Animal Care. The adrenal glands were removed and micro-dissected to isolate the medulla. The medullas were washed in HEPES buffer three times and then added to a collagenase solution (collagenase type 1: 3mg/ml, DNAase : 0.2 mg/ml and hyaluronidase: 2.4 mg/ml). The cells were incubated at 37^0C for 25 minutes and shaken every 5 minutes. The cells were triturated with a series of pipettes (each one with a tip smaller than the last) for around 20-30 times with each pipette. The cells were then incubated for another 5 minutes before triturated again and trypsin was added (1mg/ml) for a further 5 minutes of incubation at 37^0C. The cells were then triturated again and pelleted at 2800 rpm for 4 minutes. The supernatant was removed and the cells were washed with Dulbecco's modified Eagle's medium with bovine serum albumin (DMEM-BSA). The cells were then centrifuged again and washed using DMEM-BSA. After the final spin the supernatant was removed and a volume of DMEM-BSA was added to produce 10µl per dish (usually 20-30 dishes are made). The small volumes of dissociated chromaffin cells were then plated on individual glass cover slips placed in Petri-dishes for 45 minutes to 1 hour. Then the Petri-dishes were flooded with minimal essential media with 5% insulin transferring-selenium, 50 U/ml penicillin G and 50 µg/ml streptomycin (MEM-ITS). Cells were cultured for 1.5-2 hours before each experiment.

Recording catecholamine release:

Amperometric recordings were performed according to the protocols in Xu and Tse (1999) and Tang *et al.* (2005). Individual cover slips with cells were mounted onto recording chambers (ALA Scientific Instruments, Farmingdale NY) in which the cover-slip forms the bottom of the chamber. Cells were initially perfused with a standard extracellular solution made up to the following concentrations; 150mM NaCl, 2.5mM KCl, 2mM $CaCl_2$, 1mM $MgCl_2$, 8mM glucose and 10mM Hepes (adjusted to pH 7.4 with NaOH). A carbon fibre electrode was positioned to touch a chromaffin cell gently to detect the quantal release of catecholamine. Cells were stimulated using either a local perfusion of 1mM carbamylcholine chloride (carbachol; CCh) in normal Ringers solution or bath perfusion with a high potassium solution made up to the following concentrations; 102.5mM NaCl, 50mM KCl, 2mM $CaCl_2$, 1mM $MgCl_2$, 8mM glucose and 10mM Hepes (adjusted to pH 7.4 with NaOH). When a cell was stimulated with carbachol it was done so during the 10-40 second time point of a three minute recording. Amperometric signals were recorded for 5 minutes while the cell was perfused with the high potassium solution. The high extracellular potassium depolarizes the cells, causing the VGCC to open and trigger calcium-dependant release of catecholamine. Carbon fibre electrodes (CFE) were made according to the procedures found in Zhou and Misler (1995) and Zhou *et al.* (1996). A carbon fibre (with a diameter of 7µm) was threaded into a polyethylene tube (or in our case an Eppendorf micro-pipette for delivering 0.1-10µL). The plastic at the narrow tip of the Eppendorf pipette was melted over the carbon fiber and pulled so that only a thin amount of plastic covered the carbon fiber. The newly made electrode was cut to expose an un-insulated surface of carbon fiber at its tip. The other end of the Eppendorf pipette was filled with a 4M NaCl solution to make electrical contact with the head stage of an amplifier (Zhou & Misler, 1995;Zhou *et al.*,

1996). Each CFE was voltage clamped to +700mv with a VA10 amplifier (NPI electronic; Tamm, Germany). At this voltage each molecule of catecholamine released from an adjacent chromaffin cell was oxidized at the tip of the carbon fibre electrode to generate 2 electrons that could be detected as a current by the voltage-clamp amplifier. The rapid release of a package (quantum) of catecholamine, resulting from the exocytosis of an individual dense core granule, typically generates an amperometric current with the shape of an action potential (see Fig. 1B in Chapter 1). Each carbon fibre was used only two to three times and, when applicable, randomized between control and experimental conditions. Amperometric events were analyzed using the Mini Analysis Program version 6.03 (Synaptosoft Inc., Decatar, Georgia, USA). Individual events were detected using the following criteria: (1) the amplitude of events must be 3x root mean square noise, (2) the 50%-90% rise time of the spike portion must be < 5ms, (3) the decay time constant (τ) after the peak must be <40ms, (4) the interval between the peaks of two adjacent events must be > 3x the decay time of the first event, (5) the area must be larger than 10fC and (6) the half width must be greater than 1ms (Xu & Tse, 1999;Tang *et al.*, 2005).

All events that the program detected were then inspected visually. The data were further processed in Origin version 7.5 (OriginLab Corporation, Northampton, Massachusetts, USA). The mean value of each kinetic parameter of the amperometric signals were compared as follows: the mean cellular value of each parameter was obtained, then the mean cellular values from every cell for each experimental condition were averaged to calculate a "mean of cellular means" value; 2 sample t-tests were performed between the mean of cellular means of control and experimental conditions to determine statistical significance. The distribution of each kinetic parameter at different values of $Q^{1/3}$ was also compared. These comparisons involve $Q^{1/3}$, instead of Q, because when the distributions of Q values are plotted as a histogram it is skewed to the

right whereas the distribution histogram of $Q^{1/3}$ is roughly Gaussian. This is due to the fact that the diameter (rather than the volume) of the LDCGs has a roughly Gaussian distribution and the vesicular concentration of catecholamine of LDCGs in chromaffin cells is relatively constant (Gong *et al.*, 2003). A Kolmogrov-Smirnov 2 sample test on the culmitative distribution was performed to determine whether the distributions from two experimental conditions are statistically different. Kinetic parameters were also compared at matched narrow ranges of $Q^{1/3}$ values to determine if kinetic parameters were altered only at particular ranges of $Q^{1/3}$. Two sample t-tests were used for ranges of $0.1pC^{1/3}$ between the control and experimental conditions.

Fructose-fed rats:

The tissue from fructose-fed rats and age-matched controls were obtained from Professor Clanachan's lab (Department of Pharmacology) where rats were ordered at the age of 6 weeks. The protocol for fructose feeding is the addition of 10% fructose (w/v) in the drinking water for duration of 6 weeks. All experimental animals were used within 5 days after the 6^{th} week of fructose feeding. Fructose-fed rats were compared against aged-matched control rats. It is important to use aged-matched controls because the kinetics of vesicular release change with age; the area, half width and amplitude all become larger as animals become older (Elhamdani *et al.*, 2002;Zanin *et al.*, 2011).

Determination of total catecholamine content:

Total catecholamine content of the cells was determined using high pressure liquid chromatography (HPLC) with electrochemical detection which was conducted by Professor Baker's lab (Department of Psychiatry). Cells were dissociated as described above, except there was no plating of the cells. Instead after the second DMEM-BSA wash, cells were washed with

2ml of PBS solution (made up of 137mM NaCl, 27mM KCl, 101.5mM $Na_2HPO_4 \cdot 7H_2O$ and 17.6mM KH_2PO_4) and again with 1ml of PBS. The cells were transferred to a 1.5ml Eppendorf tube and spun down at 28000 rpm for 4 minutes, the supernatant was removed and the pellet of cells was frozen for storage at -80^{o}C. The cells were prepared for HPLC in the following manner: cells were re-suspended and homogenized in 100µL of Millipore-filtered water, and then a 45µL sample of the homogenate was transferred to a microfuge vial which contained 5µL of 1M perchloric acid with EDTA and ascorbic acid. The cells were vortexed and centrifuged at 10000 rpm for 4mins, and 10µL of the supernatant was used for the HPLC assay. The rest of the homogenate was used in a Pierce® BCA protein assay to standardize the catecholamine content to protein levels.

Calcium Imaging

Plated cells were incubated in 0.5ml of normal Ringer's solution and 0.5ml of 5µM Fura-2-acetoxymethyl ester (Fura-2AM) with dimethyl sulfoxide (DMSO) as carrier. Fura-2AM is a ratiometric calcium dye that is activated by esterase activity in the cell, and the AM modification allows the dye to permeate the cell membrane. The cells were incubated with the dye for 10 minutes before imaging was performed. For one set of experiments done by Dr. Amy Tse, cells were perfused with the normal Ringer's solution after incubation with the dye, and the cells were imaged at 340nm and 380nm during a 5 minute bath application of 50mM KCl. In an experiment I conducted, a local perfusion system was set up and imaging was performed using 10s of normal Ringer's followed by 30s of carbachol in normal extracellular solution. This was followed by 2mins and 20s of washout with normal Ringer's solution. The calcium concentration was quantified using the ratio of 340nm and 380nm excitation. This same procedure was also conducted using a calcium-free solution made up to the following concentrations; 150mM NaCl,

2.5mM KCl, 1mM EGTA, 3mM $MgCl_2$, 8mM glucose and 10mM Hepes (adjusted to pH 7.4 with NaOH).

Reference List:

Elhamdani A, Palfrey CH, & Artalejo CR (2002). Ageing changes the cellular basis of the "fight-or-flight" response in human adrenal chromaffin cells. *Neurobiol Aging* 23, 287-293.

Gong LW, Hafez I, Alvarez de TG, & Lindau M (2003). Secretory vesicles membrane area is regulated in tandem with quantal size in chromaffin cells. *J Neurosci* 23, 7917-7921.

Tang KS, Tse A, & Tse FW (2005). Differential regulation of multiple populations of granules in rat adrenal chromaffin cells by culture duration and cyclic AMP. *J Neurochem* 92, 1126-1139.

Xu J & Tse FW (1999). Brefeldin A increases the quantal size and alters the kinetics of catecholamine release from rat adrenal chromaffin cells. *J Biol Chem* 274, 19095-19102.

Zanin MP, Phillips L, Mackenzie KD, & Keating DJ (2011). Aging differentially affects multiple aspects of vesicle fusion kinetics. *PLoS One* 6, e27820.

Zhou Z & Misler S (1995). Action potential-induced quantal secretion of catecholamines from rat adrenal chromaffin cells. *J Biol Chem* 270, 3498-3505.

Zhou Z, Misler S, & Chow RH (1996). Rapid fluctuations in transmitter release from single vesicles in bovine adrenal chromaffin cells. *Biophys J* 70, 1543-1552.

Chapter 3 Results:

Fructose feeding robustly increases the quantal release of catecholamine from chromaffin cells stimulated with 1mM carbachol

Isolated chromaffin cells typically have a very low rate of spontaneous quantal release of catecholamine; on average less than 1 amperometric signal was detected per minute from individual un-stimulated chromaffin cells. When chromaffin cells were stimulated by local perfusion of 1 mM carbachol for 30 s, an increase in the frequency of amperometric signals could be detected for up to 3 minutes (Fig. 1). I calculated the total amount of catecholamine that was released within 3 minutes after the onset of carbachol application by integrating the amperometric current during this period (i.e. measuring the area under the entire amperometric trace). In cells isolated from fructose-fed rats this parameter was significantly increased to ~2.4-fold that of control rats (144.13±24.88 pC in the control chromaffin cells; 345.43±58.45 pC in chromaffin cells from fructose-fed rats, Fig. 2A).

Fructose feeding also increased the amount of catecholamine that was released during individual amperometric events, which reflects the quantal size (Q). In cells from fructose-fed rats the mean cellular Q was significantly increased to 137% that of control cells (0.278±0.019 pC in the control chromaffin cells; 0.381±0.022 pC in chromaffin cells from fructose-fed rats, Fig. 2B). However, the mean number of events detected per cell during the 3 minutes of recording was not significantly changed by fructose-feeding (95.68±9.29 events/cell in control chromaffin cells and 104.66±8.75 events/cell in the chromaffin cells from fructose-fed rats; Fig. 2C).

The above results raise the issue that, for the cells isolated from fructose-fed rats, the 37% increase in Q cannot fully account for the much larger increase in the total amount of catecholamine release from individual cells (~2.4-fold), if the number amperometric signals from individual cells were indeed very similar. However, it is probable that the number of "detectable" amperometric events significantly underestimated the actual number of LDCGs undergoing exocytosis adjacent to the carbon fibre electrode during the 3 minutes of recording. For both group of cells ~14% of the detected amperometric events had two or more peaks, which probably resulted from multiple LDCGs undergoing exocytosis in rapid succession (within ~50 mS). However, because I could not accurately resolve the precise number of peaks in most of these signals, each of these signals were only counted as a single "event". If the frequency of quantal release was actually increased, the above procedure is expected to further underestimate the true number of amperometric events.

I examined if the increase in Q among cells isolated from fructose fed rats was associated with certain sub-populations of amperometric signals by plotting the $Q^{1/3}$ distribution of all the non-overlapping signals from each experimental condition. The distribution of $Q^{1/3}$ was chosen because it gives a less skewed distribution (Xu *et al.*, 2005;Tang *et al.*, 2005). Fig. 3 shows that chromaffin cells from fructose-fed rats released a larger proportion of granules with $Q^{1/3} > 0.6$ $pC^{1/3}$ and a smaller proportion of granules with $Q^{1/3} < 0.6$ $pC^{1/3}$. When the data in Fig. 3 are transformed into cumulative distribution plots (Fig. 4), the cumulative curve for chromaffin cells from fructose-fed rats is right-shifted. A Kolmogrov-Smirnov test on the data in Fig. 4 shows that the cumulative distributions for the two experimental groups are significantly different ($P < 10^{-4}$).

One way to increase catecholamine release and Q in chromaffin cells is by having an increase in catecholamine synthesis leading to an increase in the total cellular amount of catecholamine in the cells. To examine this possibility I obtained assistance from the Neurochemical Research Unit in the Department of Psychiatry which has a HPLC whose output is directly connected to an instrument for electrochemical quantification of biogenic amines. Fig. 5A shows the average total amounts of catecholamine (normalized to the amount of cellular proteins) in the entire population of cells (mostly chromaffin cells) isolated from the adrenal medulla of control rats and fructose-fed rats were not significantly different (Fig. 5A). Moreover, the ratio of adrenalin to noradrenalin in these cells was also not significantly changed by fructose feeding (Fig. 5B). In fact fructose-feeding caused no significant difference in either the total cellular amount or relative abundance of the following biogenic amines or their acidic metabolites: adrenalin, noradrenalin, dopamine, 5-hydroxytryptamine (serotonin), homovanillic acid, 3,4-dihydroxyphenylacetic acid, and 5-hydroxyindoleacetic acid.

Another way to increase catecholamine secretion and Q is to increase the influx of Ca^{2+} into the cell via the opening of voltage-gated Ca^{2+} channels, or through release of internal Ca^{2+} stores (Elhamdani et al., 1998). I examined this possibility by imaging the change in $[Ca^{2+}]_i$ with the ratiometric fluorescent dye fura-2 (Paredes *et al.*, 2008).The rise in $[Ca^{2+}]_i$ when the chromaffin cells were stimulated for 30 s with focal application of 1mM carbachol was essentially identical between chromaffin cells from control rats and chromaffin cells from fructose-fed rats (Fig. 6A). The mean time integral of the change in $[Ca^{2+}]_i$ when the cells are stimulated with 1mM carbachol for 30 s, followed by 2.5 min of washing, was significantly decreased in the chromaffin cells from fructose-fed rats by ~18% (32115±1132 nM·s in the control cells and 26324±1385 nM·s in the cells from fructose-fed rats; Fig. 6B). There is no

change in the magnitude of the rise in calcium from the chromaffin cells from fructose-fed and control rats. The chromaffin cells from the fructose-fed rats also had a lower change in $[Ca^{2+}]_i$ than the chromaffin cells from the control rats, which indicates that the increase in quantal size is not due to an increase in the calcium signal.

When I analyzed the kinetic parameters of individual (non-overlapping) amperometric signals, the following 5 changes were detected in cells isolated from fructose-fed rats. First the mean cellular spike amplitude of signals from cells was significantly increased by 57% (41.35±4.01 pA in control cells vs. 64.88±5.54 pA in cells from fructose-fed rats) (Fig. 7A). Second, the mean cellular spike half width was deceased by ~20% (6.45±0.23 ms in control cells vs. 5.15±0.19 ms in cells from fructose-fed rats) (Fig. 7B). Third, the mean cellular rise time was decreased by ~20% (1.50±0.06ms in control chromaffin cells vs. 1.19±0.04 ms in cells from fructose-fed rats) (Fig. 7C). Fourth, the mean cellular decay time constant τ, was decreased by 21% (11.06±0.56ms in control cells vs. 8.57±0.37 ms in cells from fructose-fed rats (Fig. 7D). Fifth, the mean cellular foot amplitude was increased by ~54% (14.31±1.53 pA in control cells vs. 22.07±1.73 pA in cells from fructose-fed rats (Fig. 8A). In contrast, one parameter of the amperometric signal, the mean cellular foot duration, was not significantly changed by fructose-feeding (5.27±0.20ms for control cells and 4.89±0.20ms for cells from fructose-fed rats) (Fig. 8B).

Previous studies had shown that, even for chromaffin cells from control rats, the kinetic parameters of individual amperometric signals varied with Q and followed certain trends (Tang et al., 2007). For example, signals with a larger Q tend to have taller amplitudes for the foot signal and the spike, as well as longer durations in foot duration, spike half-width and decay τ.

Because fructose feeding also resulted in a ~37% increase in the mean cellular value of Q, this change not only may directly contribute to some of the changes in the kinetic parameters which are shown in Fig. 8 , but may also obscure other changes in certain kinetic parameters (which are not primarily associated with the increase in Q). To clarify this issue, I analysed how fructose feeding affected each of the above kinetic parameters when the comparison was restricted to narrow and matched ranges of $Q^{1/3}$(Tang et al., 2007). For this analysis, the data sets from both experimental conditions were first sorted in an ascending value of $Q^{1/3}$, and then binned with a bin width of 0.1 $pC^{1/3}$; bins with at the lowest and highest ranges of $Q^{1/3}$ that had less than 100 events (70 events for parameters of the foot signal) were excluded from this comparison. Figs. 9 to13 showed that, for all the parameters whose cellular mean values were significantly altered by fructose feeding (i.e. a larger spike amplitude, a shorter half-width, rise time and decay τ, as well as a larger foot amplitude), a significant change in the same direction was also detected at least within the matched ranges of $Q^{1/3}$ from 0.3 to 0.7 $pC^{1/3}$; this entire range included the vast majority of amperometric signals. For some of the above parameters, fructose feeding also caused significant change for $Q^{1/3}$ as small as 0.2 $pC^{1/3}$ or as large as 1.0 $pC^{1/3}$. Fig. 14 shows that for the parameter of foot duration, whose mean cellular value was not significantly changed by fructose-feeding, between the match ranges of $Q^{1/3}$ from 0.4 to 0.8 $pC^{1/3}$ this parameter was significantly decreased by fructose feeding.

The overall patterns of changes in the kinetic parameters of individual amperometric signals shown in Figs.9-14 suggest that fructose feeding not only increased the rate of release of catecholamine during the entire rising phase of the amperometric signal, but probably also accelerated the onset of rapid fusion pore dilation and the depletion of granular catecholamine after the onset of rapid fusion pore dilation.

Fructose feeding resulted in different patterns of change in quantal release of catecholamine when chromaffin cells were stimulated by elevating extracellular K^+ ($[K^+]_{ext}$) to 50mM

When chromaffin cells were stimulated with carbachol, the increase in quantal catecholamine release and Q, as well as the accelerated kinetics of individual amperometric signals that were associated with fructose feeding seemed to involve neither an increase in the cellular content of catecholamine, nor the change in the amplitude of the rise in $[Ca^{2+}]_i$. This raised the possibility that fructose feeding might change other aspects, such as the pool size of certain classes of releasable LDCGs, the packaging of catecholamine into LDCGs, and/or properties of the fusion pore. Fructose feeding may regulate such aspects before the cells are stimulated, as well as via mechanisms that are only activated after the activation of ACh receptors (AChRs). Furthermore, because chromaffin cells express not only ionotropic nAChRs, but also metabotropic mAChRs, some of the effects of fructose feeding described in the previous section may involve changes in the cellular messengers that are generated by the activation of mAChRs. To assess the relative contributions of some of the above possibilities, I examined whether certain effects of fructose feeding described in the previous section could be reproduced when chromaffin cells were stimulated by elevating $[K^+]_{ext}$, which is expected to bypass the activation of AChRs, but directly depolarize the cell, and hence activate VGCCs to trigger quantal catecholamine release. My preliminary studies have shown that when chromaffin cells were stimulated by elevating $[K^+]_{ext}$ to 50 mM the frequency of amperometric signals recorded during 5 minutes of this stimulus was sufficient for analysis of their kinetic parameters (see Chapter 1 Fig. 1A).

Contrary to the results of my experiments which employed carbachol to stimulate the cells, when chromaffin cells from fructose-fed rats were stimulated by elevating $[K^+]_{ext}$ to 50 mM for 5 minutes, the total amount of catecholamine released from individual cells (which was determined from the time integral of the entire amperometric trace) was not significantly different from that of control cells (426.13±43.79pC for the control cells vs. 432.55±68.32pC for cells from fructose-fed rats) (Fig. 15A). More importantly, with this stimulus, the mean cellular value of Q in cells from fructose-fed rats was significantly decreased by 19% (0.402±0.018pC in control cells vs. 0.327±0.020pC in cells from fructose-fed rats (Fig. 15B), and the mean number of events per cell was significantly reduced by 21% (300.5±17.2 events/cell in control cells vs. 237.5±15.8 events/cell in cells from fructose-fed rats (Fig. 15C). When the distribution of $Q^{1/3}$ was compared, cells from fructose-fed rats have a larger proportion of events with $Q^{1/3} < 0.7$ $pC^{1/3}$ and a smaller proportion of events with $Q^{1/3} > 0.7$ $pC^{1/3}$ (Fig. 16). The cumulative distribution of $Q^{1/3}$ shows that the curve is shifted to the left for the cells from fructose-fed rats; the Kolmogrov-Smirnov test on these sets of data shows that these two curves are significantly different ($P<1*10^{-4}$) (Fig.17). Overall, the above data indicate that the increases in quantal release of catecholamine and Q associated with fructose feeding were not reproduced when the stimulus was changed from carbachol to elevated $[K^+]_{ext}$.

Previous studies (Elhamdani et al., 1998) have reported that a reduction in the rise in $[Ca^{2+}]_i$ during the stimulus can result in a reduction in both the frequency of amperometric signals and Q. Therefore, with the help of Prof. Amy Tse, I examined whether fructose feeding affected the rise in $[Ca^{2+}]_i$ when the cell was stimulated with 50 mM K^+. As summarized in Fig. 18, fructose feeding affected neither the basal $[Ca^{2+}]_i$ nor the peak $[Ca^{2+}]_i$ when the chromaffin

cells were stimulated with 50 mM K^+; moreover the $[Ca^{2+}]_i$ after 5 minutes of 50mM K^+ stimulation was also unchanged.

To assess whether stimulation with 50 mM K^+ reproduced any of the changes in kinetic parameters of individual amperometric signals that are seen with carbacol stimulation as a result of fructose feeding, I repeated the analyses previously shown in Figs. 7 to 14. The results of such analyses on 50 mM K^+-stimulated cells are summarized in Table 1 and Figs. 19 to 26. With this stimulation, fructose feeding significantly affected the mean cellular value of only two parameters: the amplitude of both the spike (Fig. 19) and foot signal (Fig. 20) were decreased by 25% and 23%, respectively. These changes are consistent with the 19% decrease in the mean cellular value of Q (Fig. 15). When the kinetic parameters were compared at matched narrow ranges of $Q^{1/3}$ (Figs. 21 to 26), except for the foot duration (Fig. 26), fructose feeding caused significant differences in every parameter at $Q^{1/3} > 0.6$ $pC^{1/3}$ (Figs. 21-25; note that for some parameters, significant differences were also found at lower ranges of $Q^{1/3}$, for example for the spike half-width only the range between 0.3 to 0.4 $pC^{1/3}$ had no significant difference). For each of the 4 kinetic parameters which showed any significant change with fructose feeding at matched $Q^{1/3}$, the direction of change was always the same for every relevant range of $Q^{1/3}$; specifically, the spike and foot amplitudes were decreased, while the half-width, rise time and decay τ of the spike were increased. The above analysis indicates that when chromaffin cells were stimulated by 50 mM K^+, fructose feeding not only decreased Q, but also slowed down the kinetics of amperometric signals with a $Q^{1/3}$ that is larger than the modal value of ~0.6 $pC^{1/3}$.

Tables:

Table 1: Mean cellular values of kinetic parameters for chromaffin cells from fructose-fed and control rats stimulated with 50mM $[K^+]_{ext}$

Kinetic Parameter	Control N=88 cells	Fructose-fed N=68 cells
Amplitude (pA)	56.16±3.30	41.78±3.13*
Half Width (ms)	5.75±0.17	5.87±0.20
Rise Time (ms)	1.22±0.03	1.25±0.03
Decay Tau (ms)	9.72±0.30	9.87±0.33
Foot Amplitude (pA)	19.51±1.01	14.95±0.95*
Foot Duration (ms)	5.41±0.15	5.13±0.15

* $p<0.05$ for all tables and figures unless otherwise stated.

Note: errors shown here and the error bars shown in all the graphs in this paper are the standard error. All the statistics, unless otherwise stated, were done using a Student's t-test.

Figures:

Figure 1:

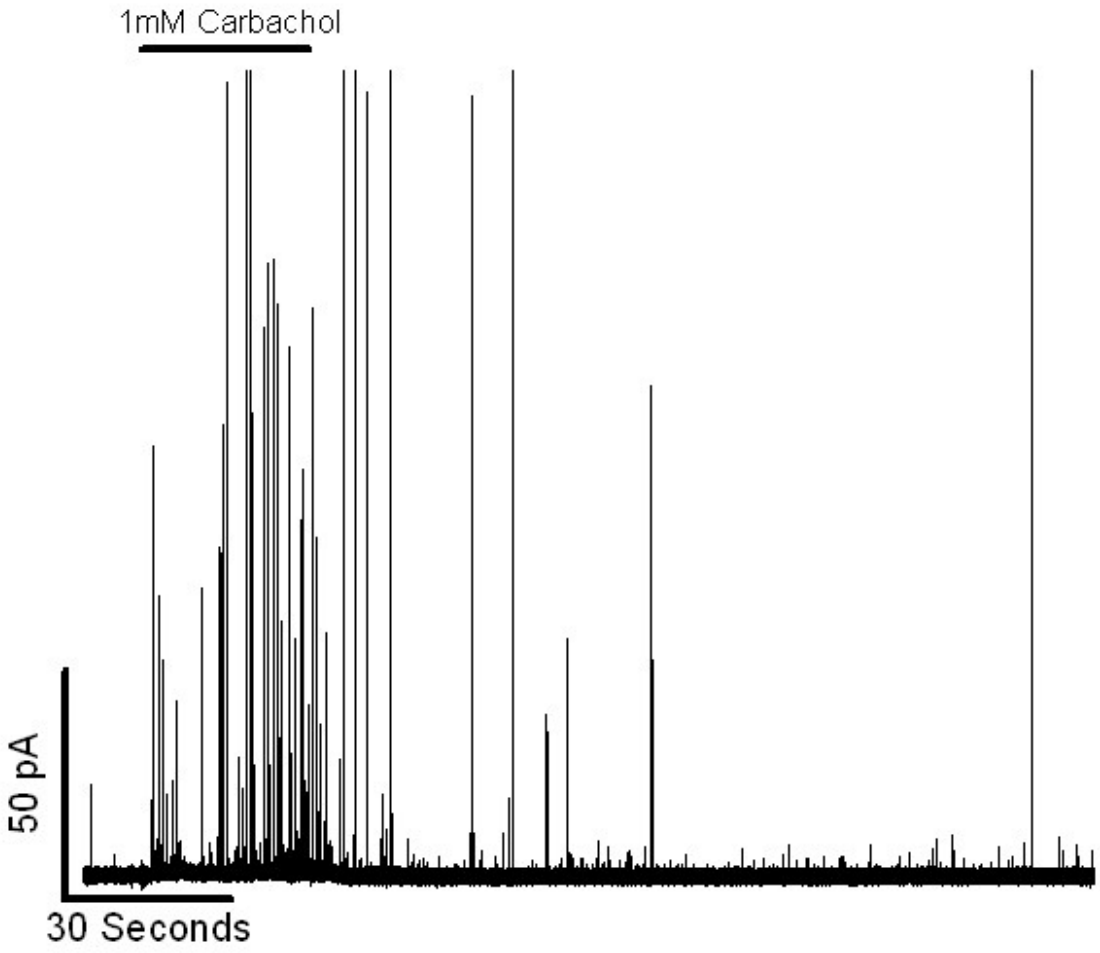

A control cell stimulated with 1mM carbachol for 30s at the begining of a 3 minute recording.

Figure 2:

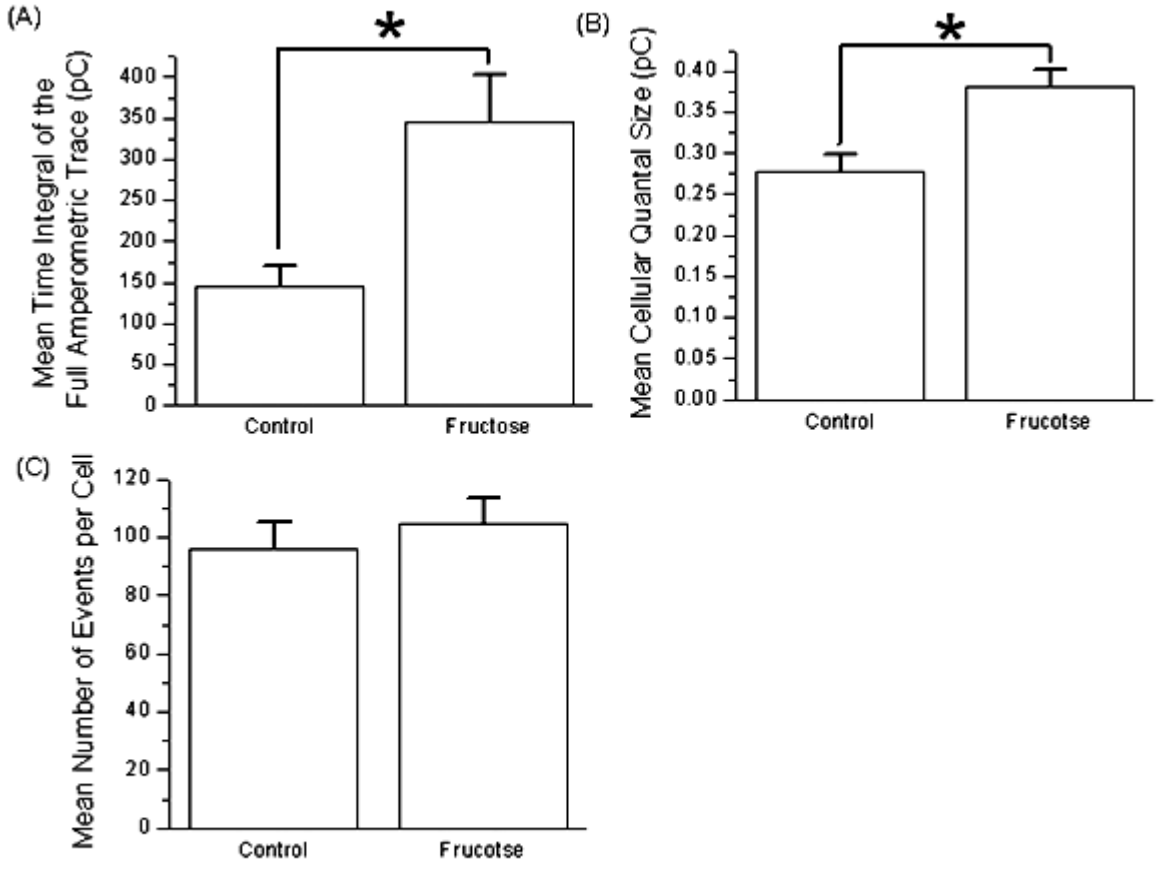

The mean time integral, taken from cells with a flat baseline (A). The mean cellular quantal size (Q) for control cells and cells from fructose-fed animals was calculated by taking the mean value of Q from individual cells and then taking the mean of the means Q from each cell in an experimental group (B). The mean number of events per cell was calculated by taking the mean of the number of events detected by amperometry in three minutes from individual cells (C). N= 47 cells from three rats for the controls and 44 cells from three fructose-fed rats

Figure 3:

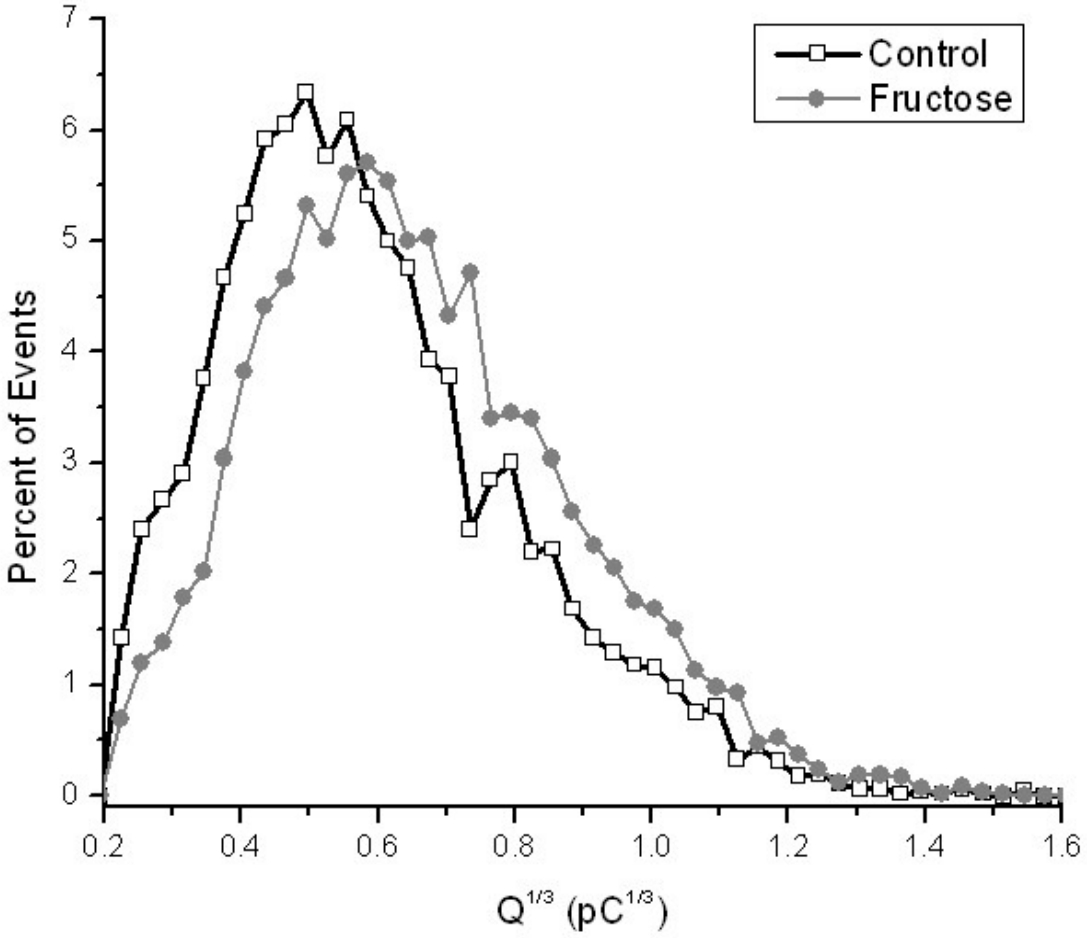

The distribution of events with the cube root of Q for control cells and cells from fructose-fed rats. N= 4497 events for the controls and 4605 events for the fructose-fed rats.

Figure 4:

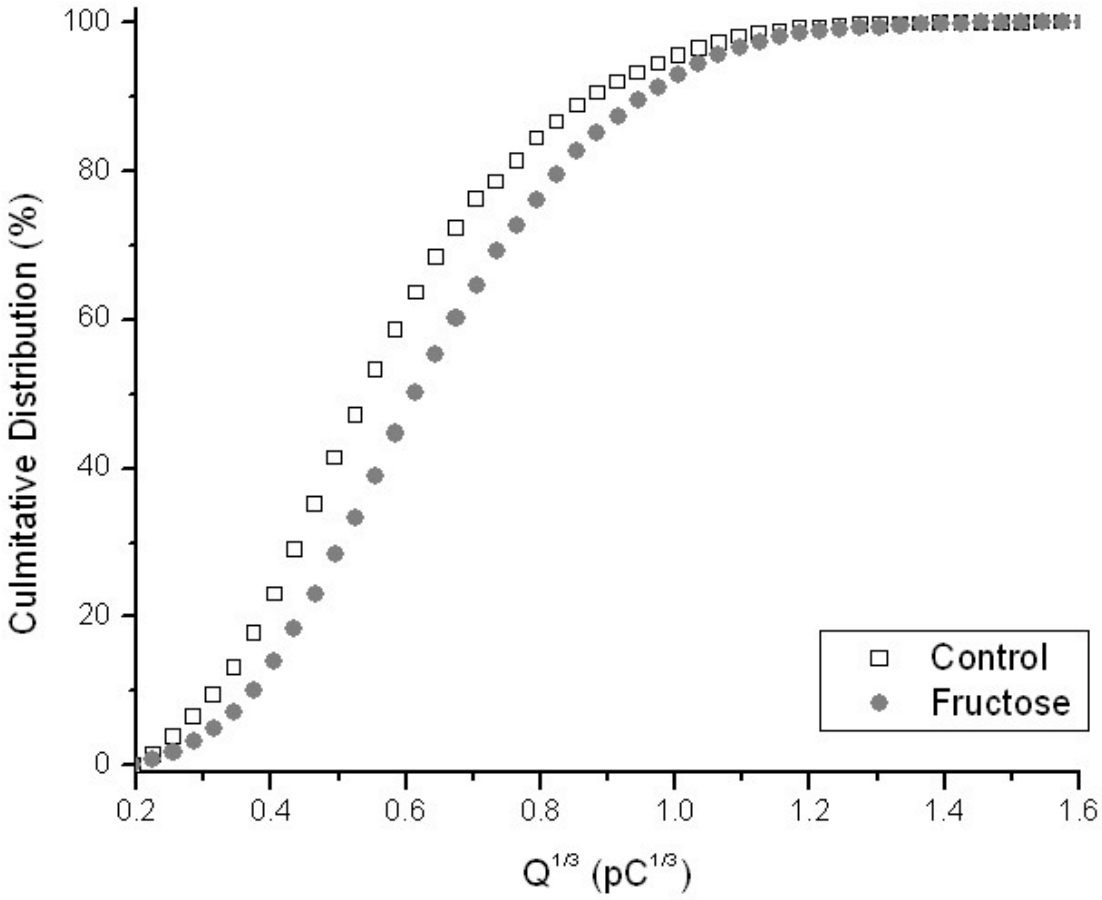

The Kolmogrov-Smirnov test on the cumulative distribution gives a $p<1X10^{-4}$. N= 4497 events for the controls and 4605 events for the fructose-fed rats.

Figure 5:

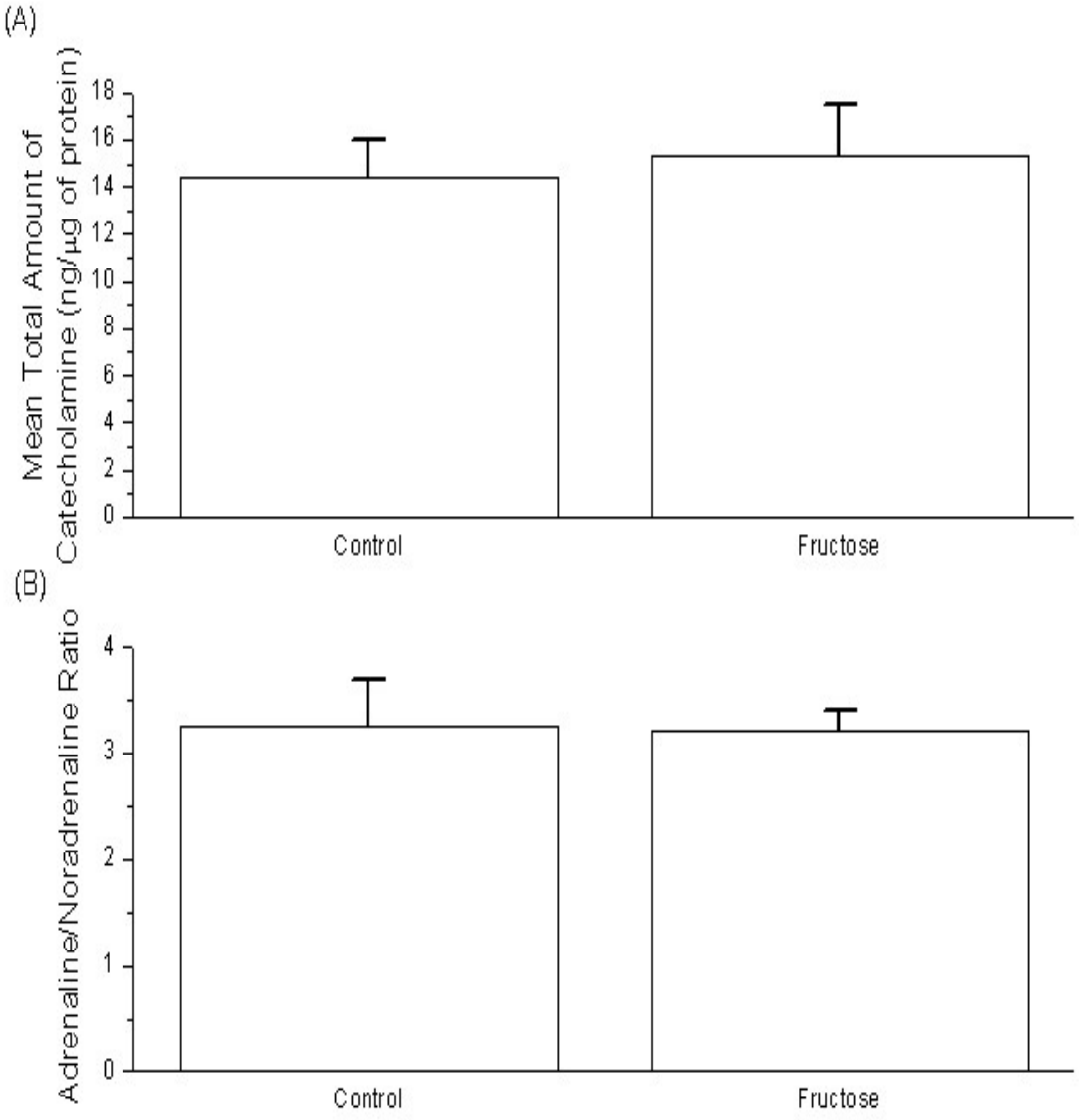

The mean total catecholamine (A) and adrenalin to noradrenalin ratio (B) was taken using HPLC on populations of cells from rat adrenal medullas. N= 6 rats for each condition.

Figure 6:

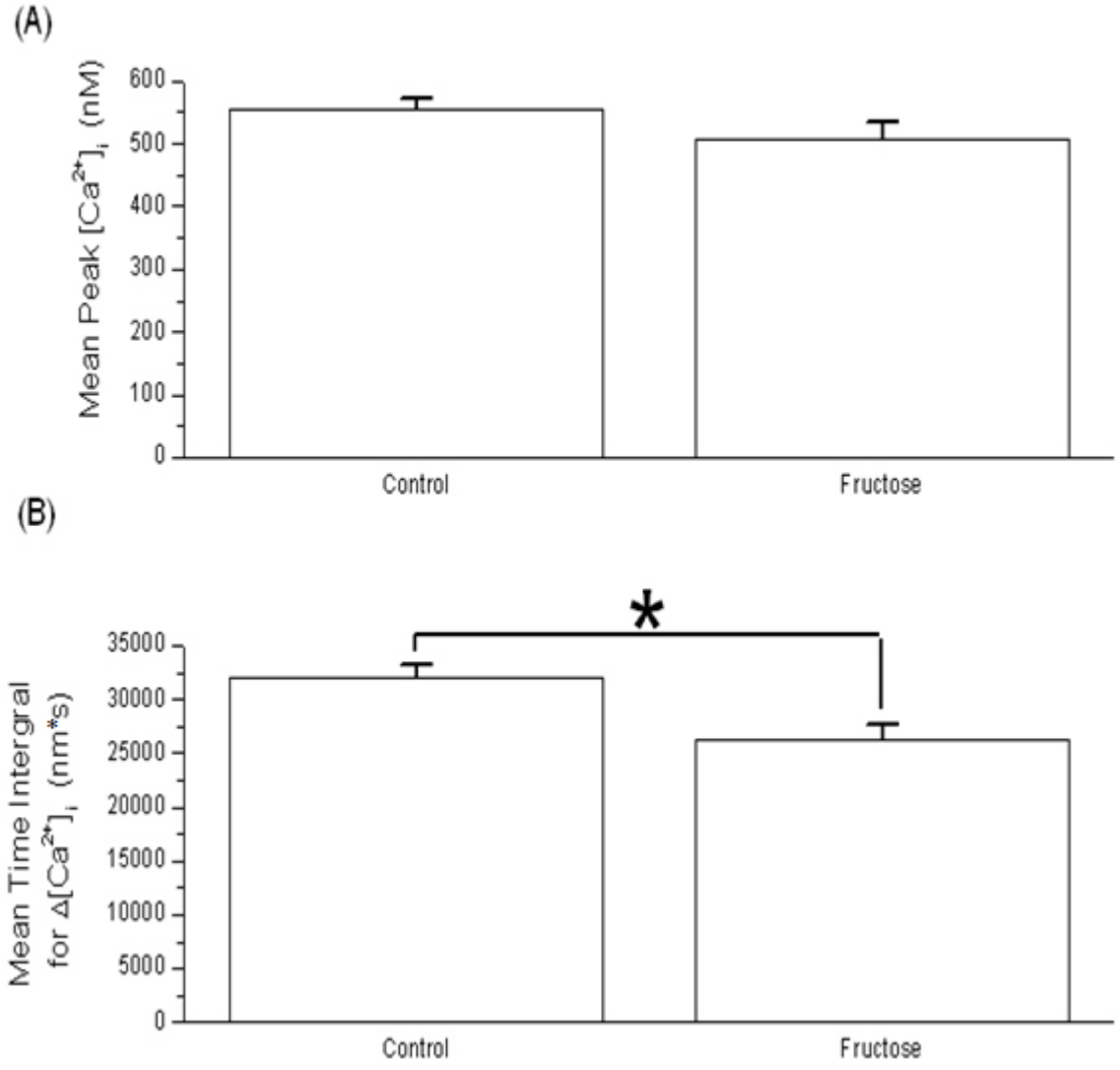

The mean peak internal calcium concentration when cells are stimulated with 1mM carbachol for 30s (A).The mean time integral when cells are stimulated with 1mM carbachol for 30s followed by 2.5min of washing (B). N= 50 cells and 46 cells from two control rats and one fructose-fed rat respectively.

Figure 7:

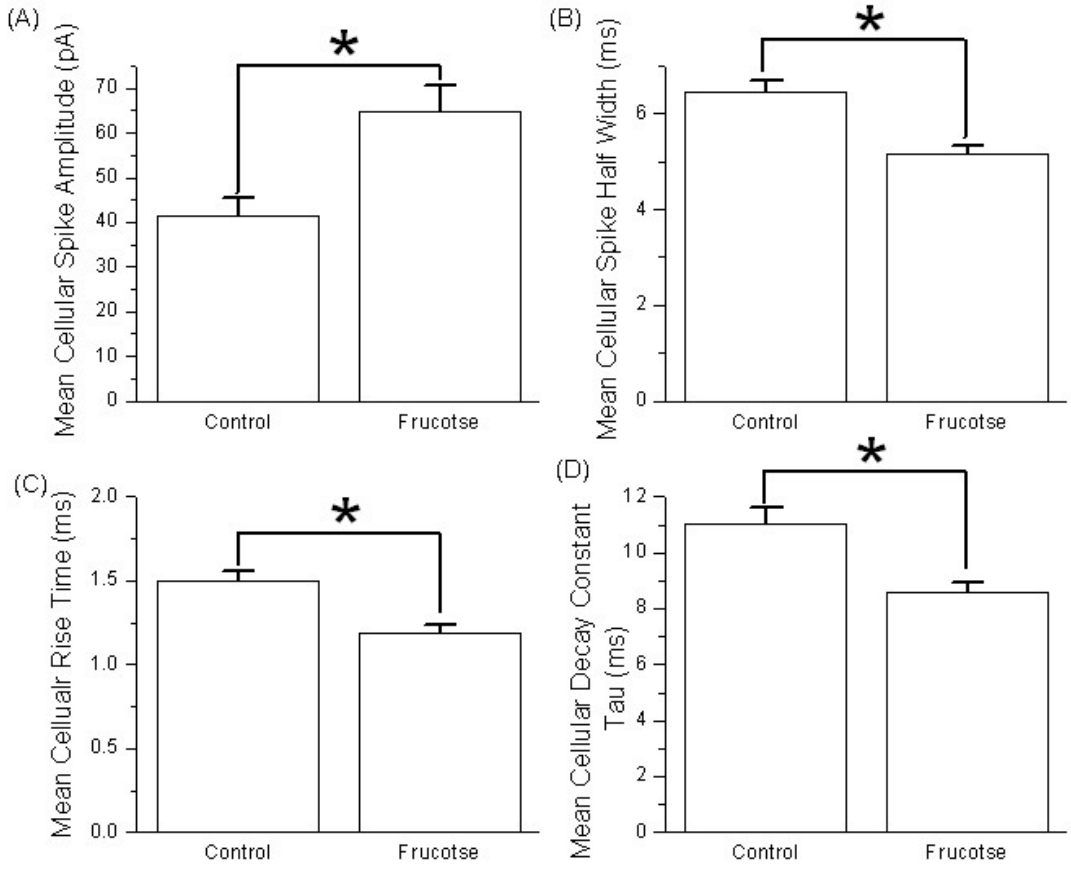

The mean cellular spike amplitude (A), the mean cellular spike half width (B), the mean cellular rise time (C) and the mean cellular decay time constant τ (D). N= 47 cells from three rats for the controls and 44 cells from three fructose-fed rats.

Figure 8:

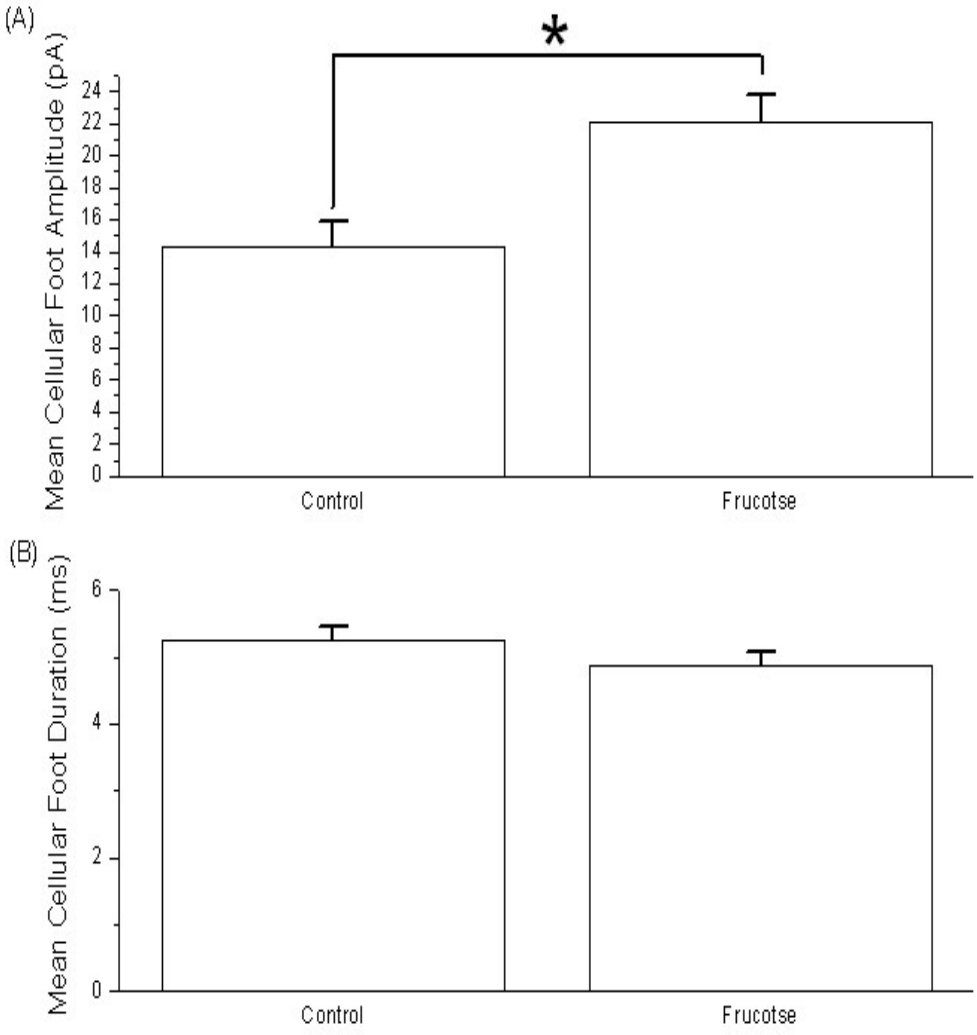

The mean cellular foot amplitude (A) and the mean cellular foot duration (B). N= 47 cells from three rats for the controls and 44 cells from three fructose-fed rats.

Figure 9:

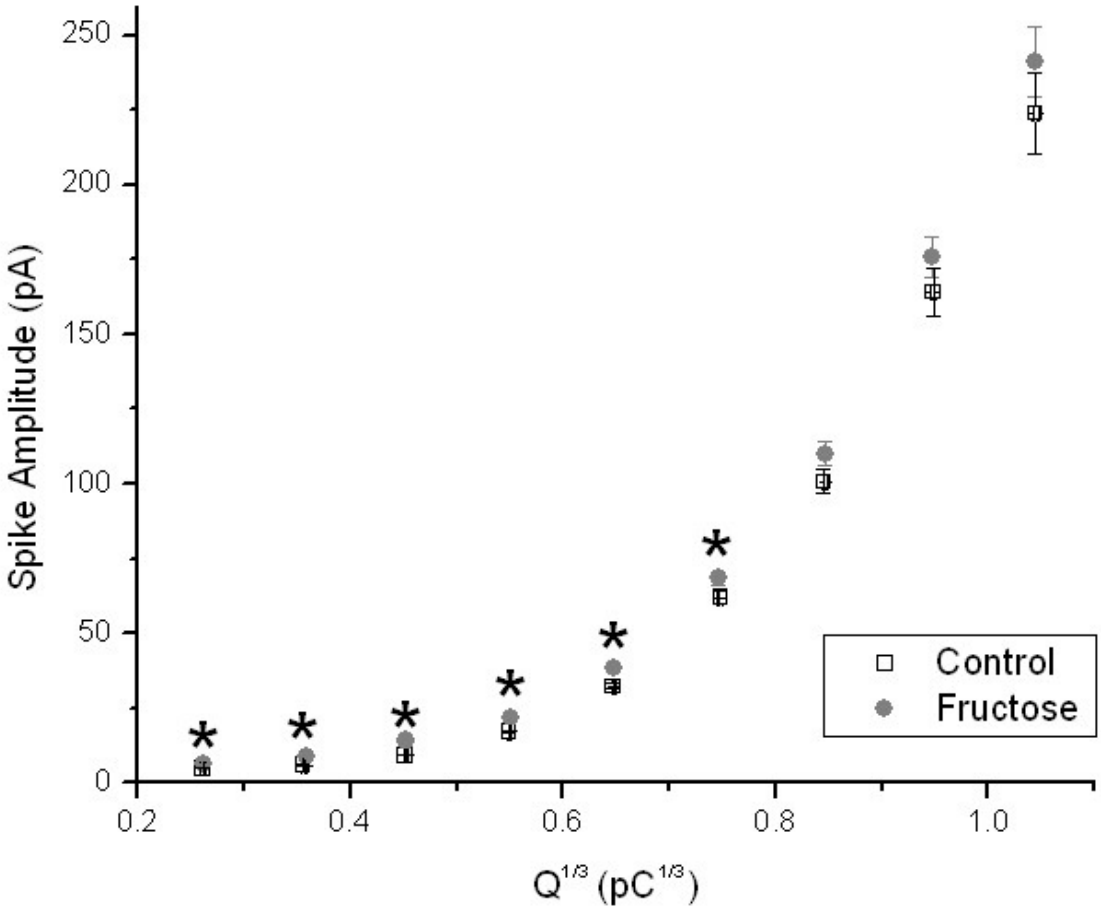

The spike amplitude at matched bin size of 0.1 $pC^{1/3}$. Bins with less than 100 events were excluded. N= 4497 events for the controls and 4605 events for the fructose-fed rats.

Figure 10:

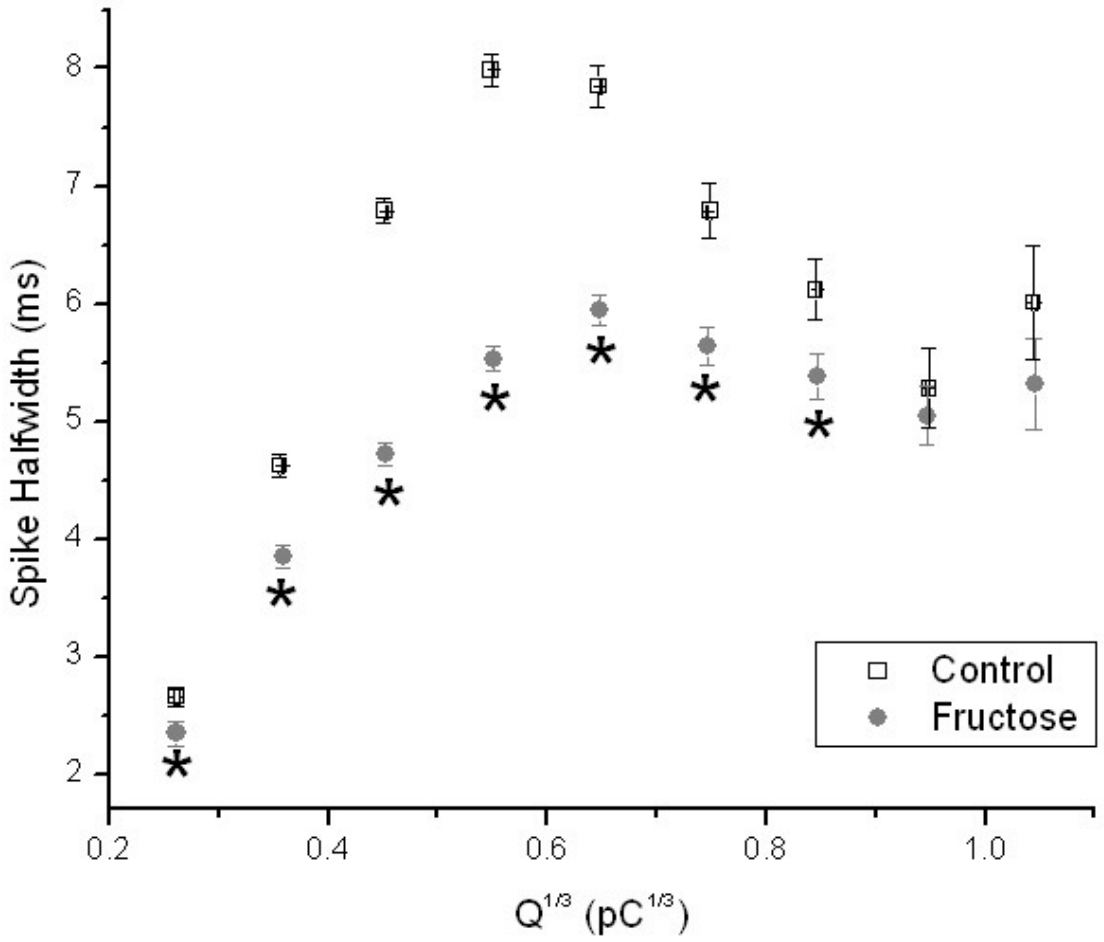

The spike half width at matched bin size of 0.1 $pC^{1/3}$. Bins with less than 100 events were excluded. N= 4497 events for the controls and 4605 events for the fructose-fed rats.

Figure 11:

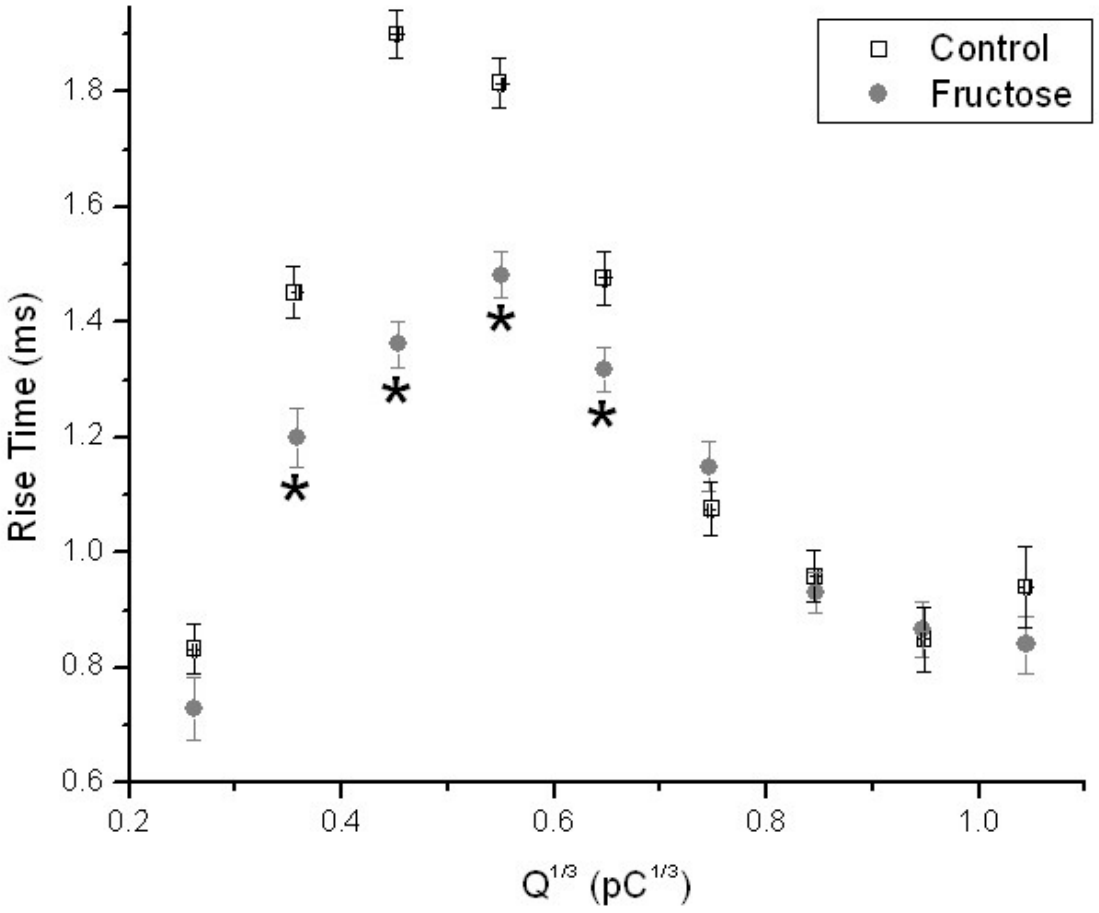

The 50-90% rise time at matched bin size of 0.1 $pC^{1/3}$. Bins with less than 100 events were excluded. N= 4497 events for the controls and 4605 events for the fructose-fed rats.

Figure 12:

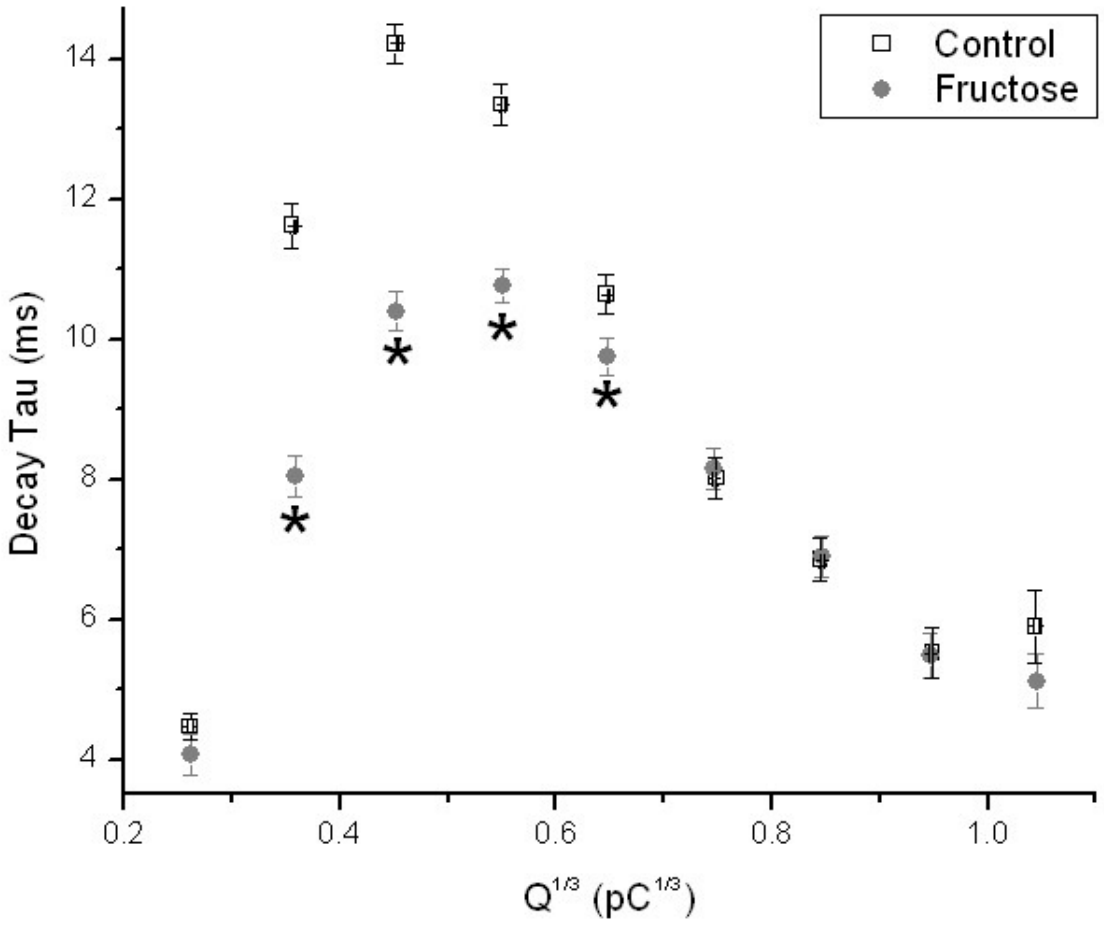

The decay time constant τ at matched bin size of 0.1 $pC^{1/3}$. Bins with less than 100 events were excluded. N= 4497 events for the controls and 4605 events for the fructose-fed rats.

Figure 13:

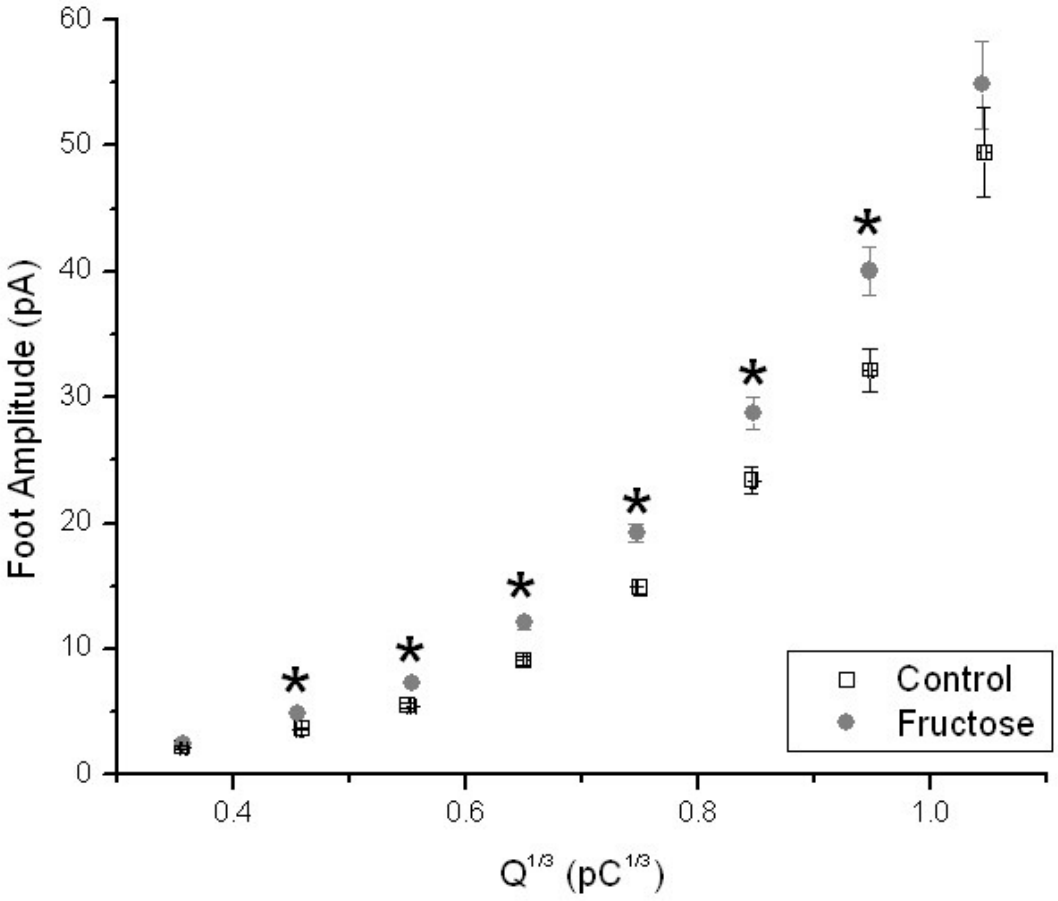

The foot amplitude at matched bin size of 0.1 $pC^{1/3}$. Bins with less than 70 events were excluded. N= 2243 events for the controls and 2240 events for the fructose-fed rats.

Figure 14:

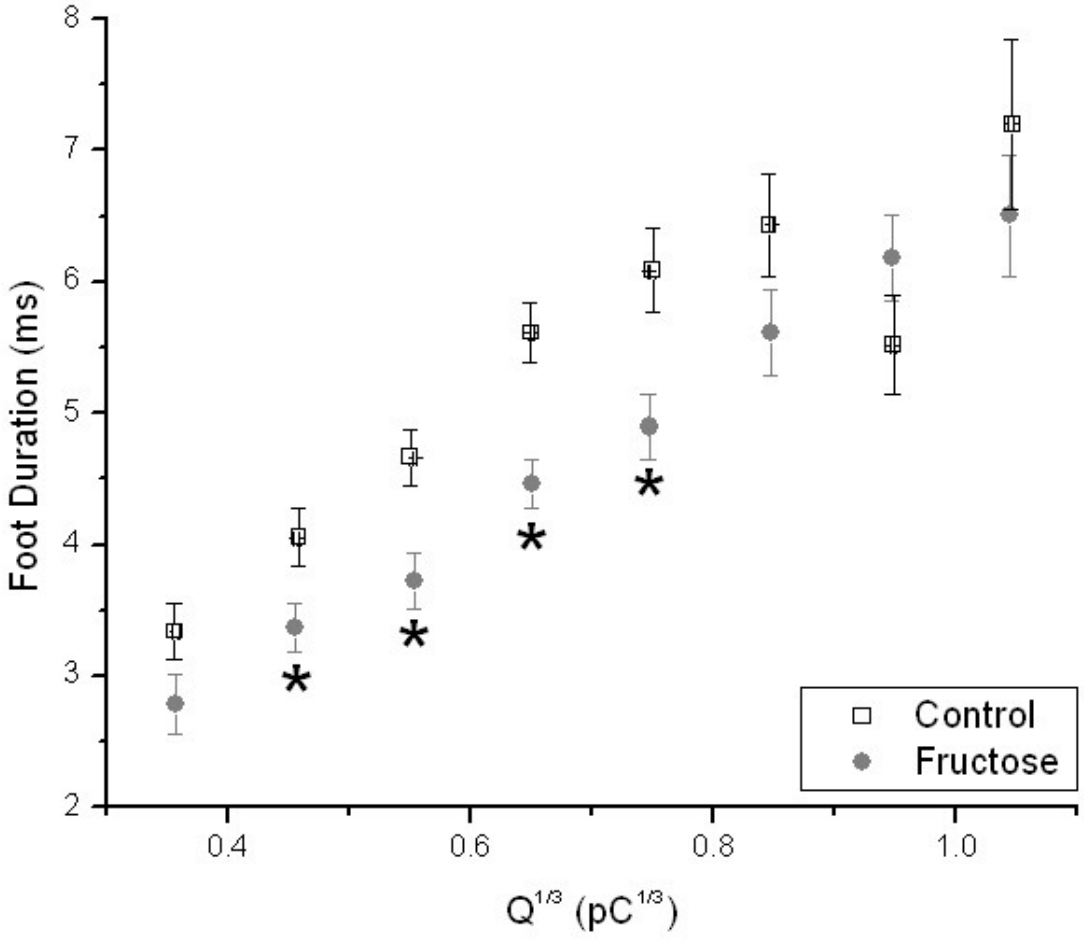

The foot duration at matched bin size of 0.1 $pC^{1/3}$. Bins with less than 70 events were excluded. N= 2243 events for the controls and 2240 events for the fructose-fed rats

Figure 15:

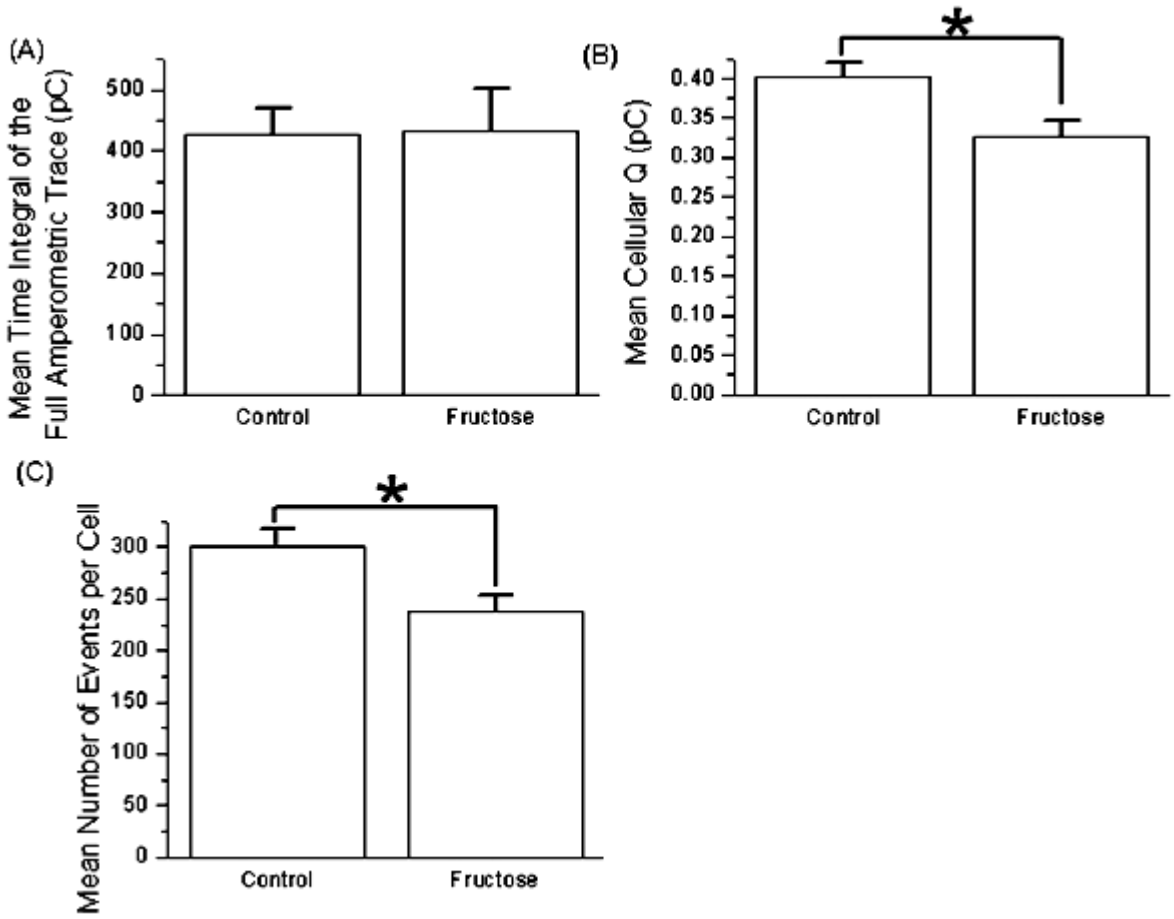

The mean time integral, taken from cells with a flat base line (A). The mean cellular quantal size (Q) (B). The mean number of events per cell was calculated by taking the mean of the number of events detected by amperometry in five minutes from individual cells (C). N= 88 cells from five rats for the controls and 68 cells from four fructose-fed rats

Figure 16:

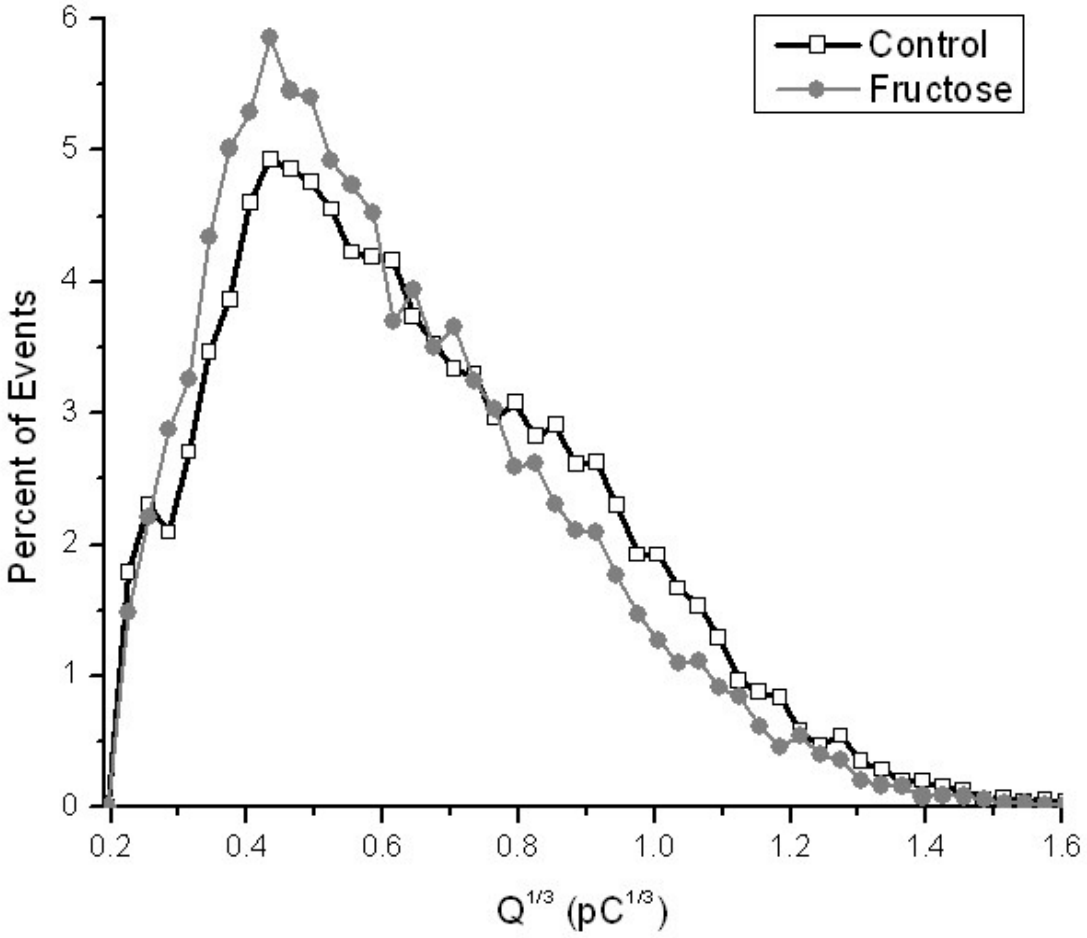

The distribution of events with the cube root of Q for control cells and cells from fructose-fed rats. N= 26434 events for the controls and 16151 events for the fructose-fed rats.

Figure 17:

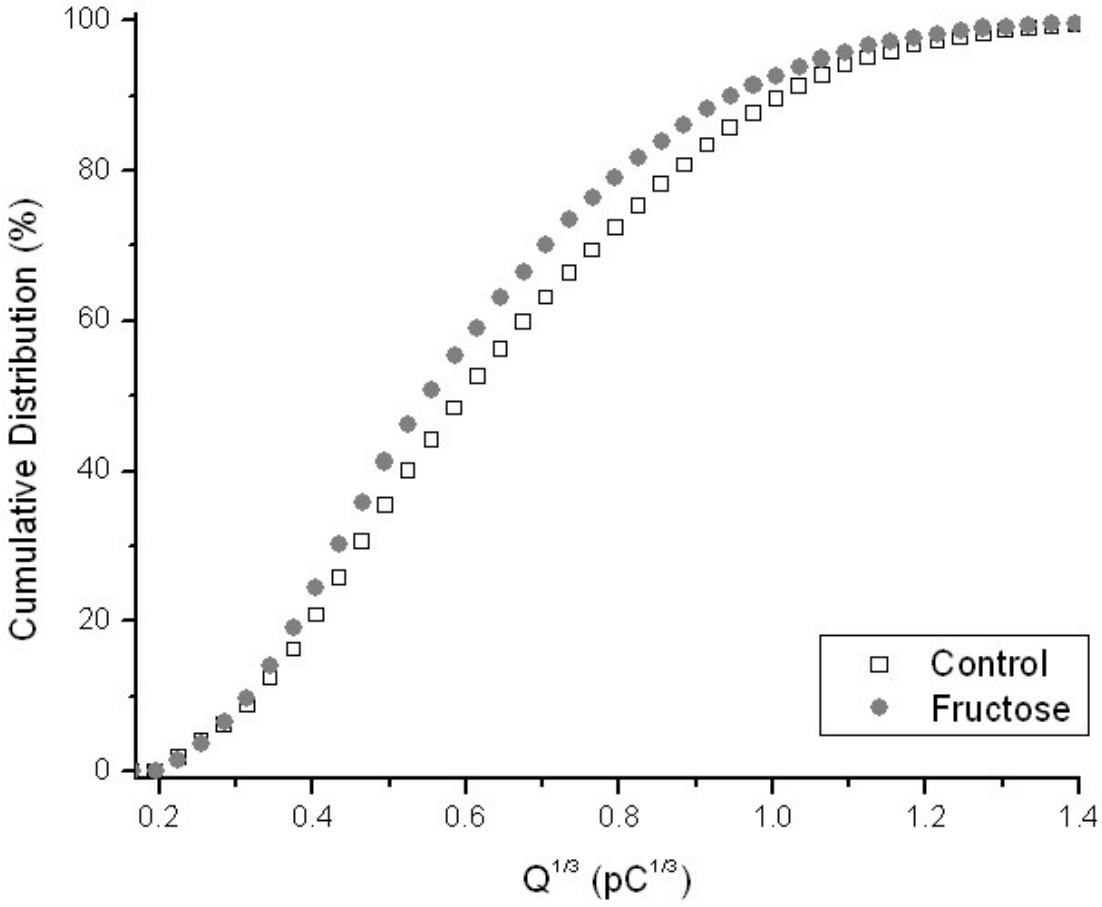

The Kolmogrov-Smirnov test on the cumulative distribution gives a $p<1X10^{-4}$. N= 26434 events for the controls and 16151 events for the fructose-fed rats.

Figure 18:

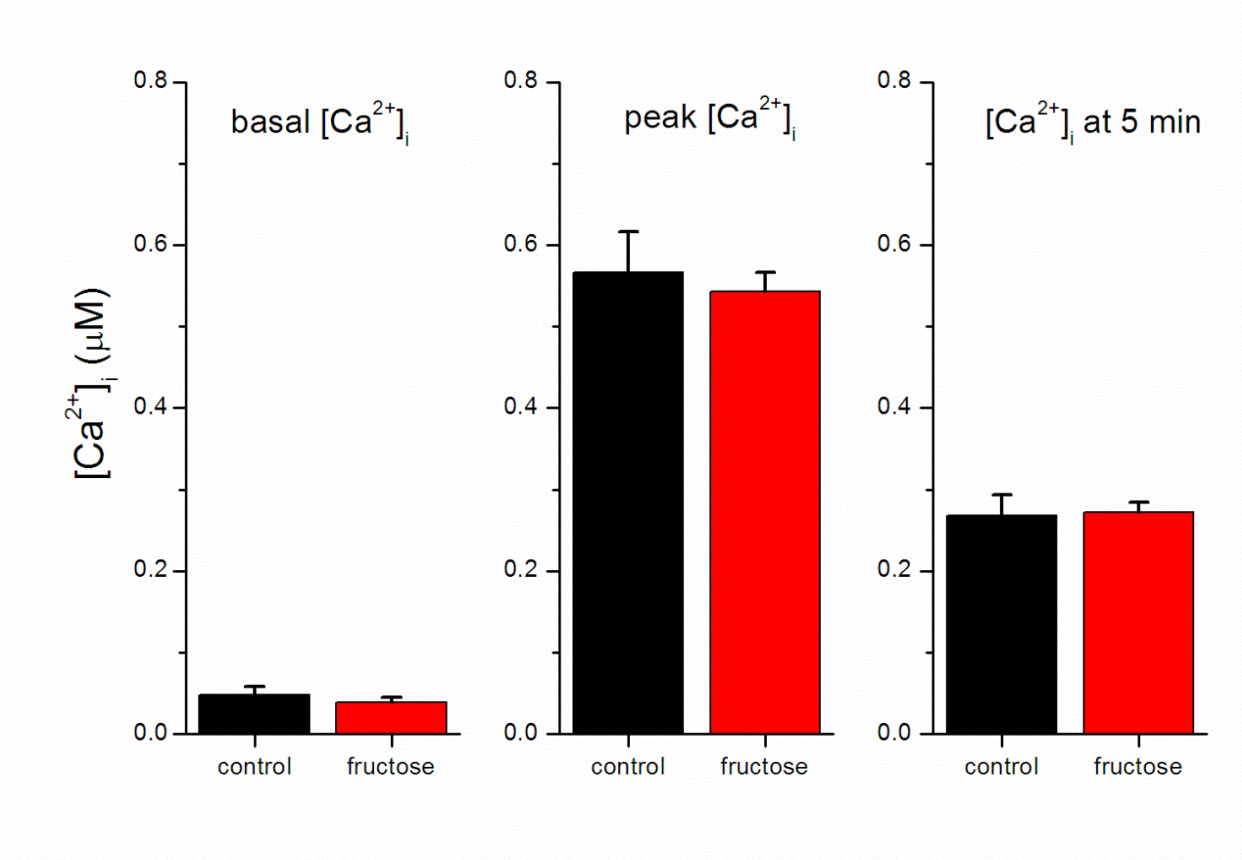

The first panel depicts the basal $[Ca^{2+}]_i$ before stimulation, the second panel is the peak $[Ca^{2+}]_i$ after stimulation with 50mM KCl, and the third panel is the $[Ca^{2+}]_i$ after 5 minutes of KCl perfusion. N=31 cells for the basal and peak $[Ca^{2+}]_i$ and 30 cells for the $[Ca^{2+}]_i$ after five minutes of 50mM KCl perfusion.

Figure 19:

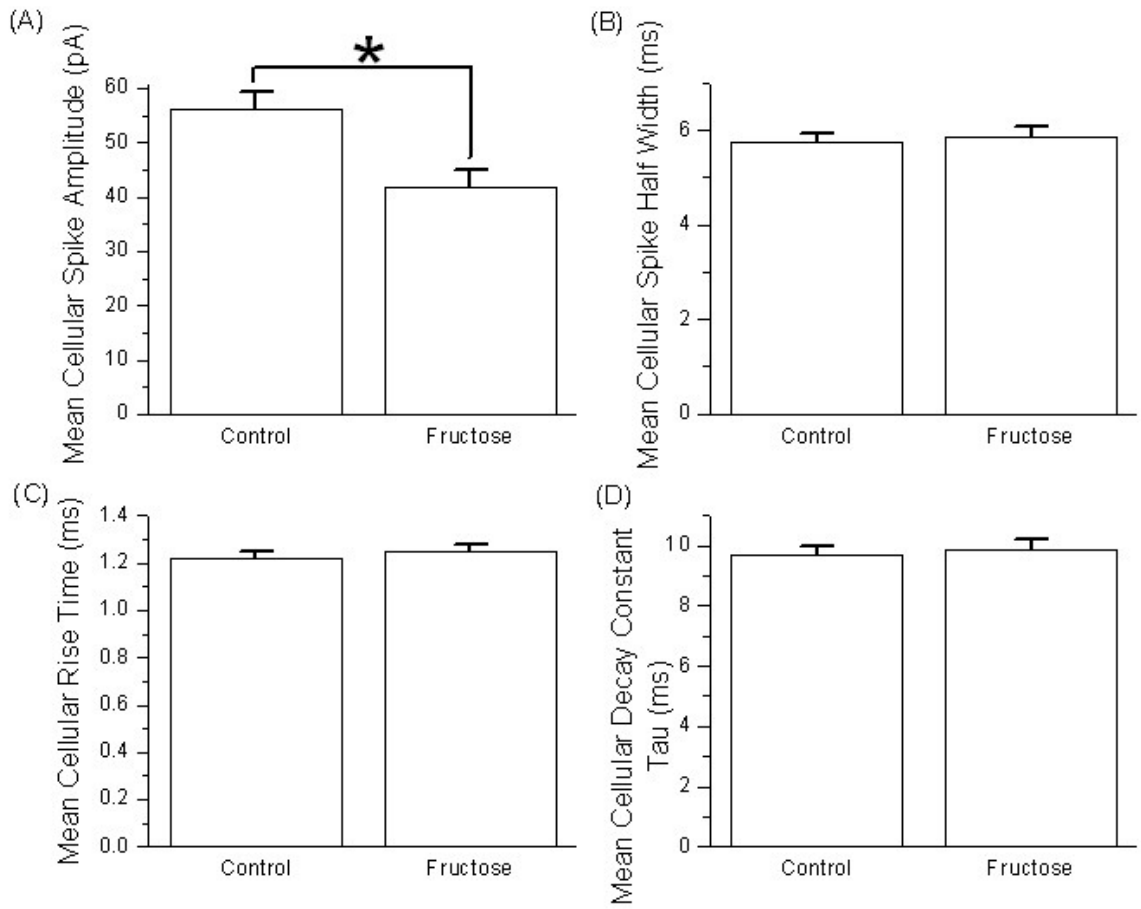

The mean cellular spike amplitude (A), the mean cellular spike half width (B), the mean cellular rise time (C) and the mean cellular decay time constant τ (D). N= 88 cells from five rats for the controls and 68 cells from four fructose-fed rats.

Figure 20:

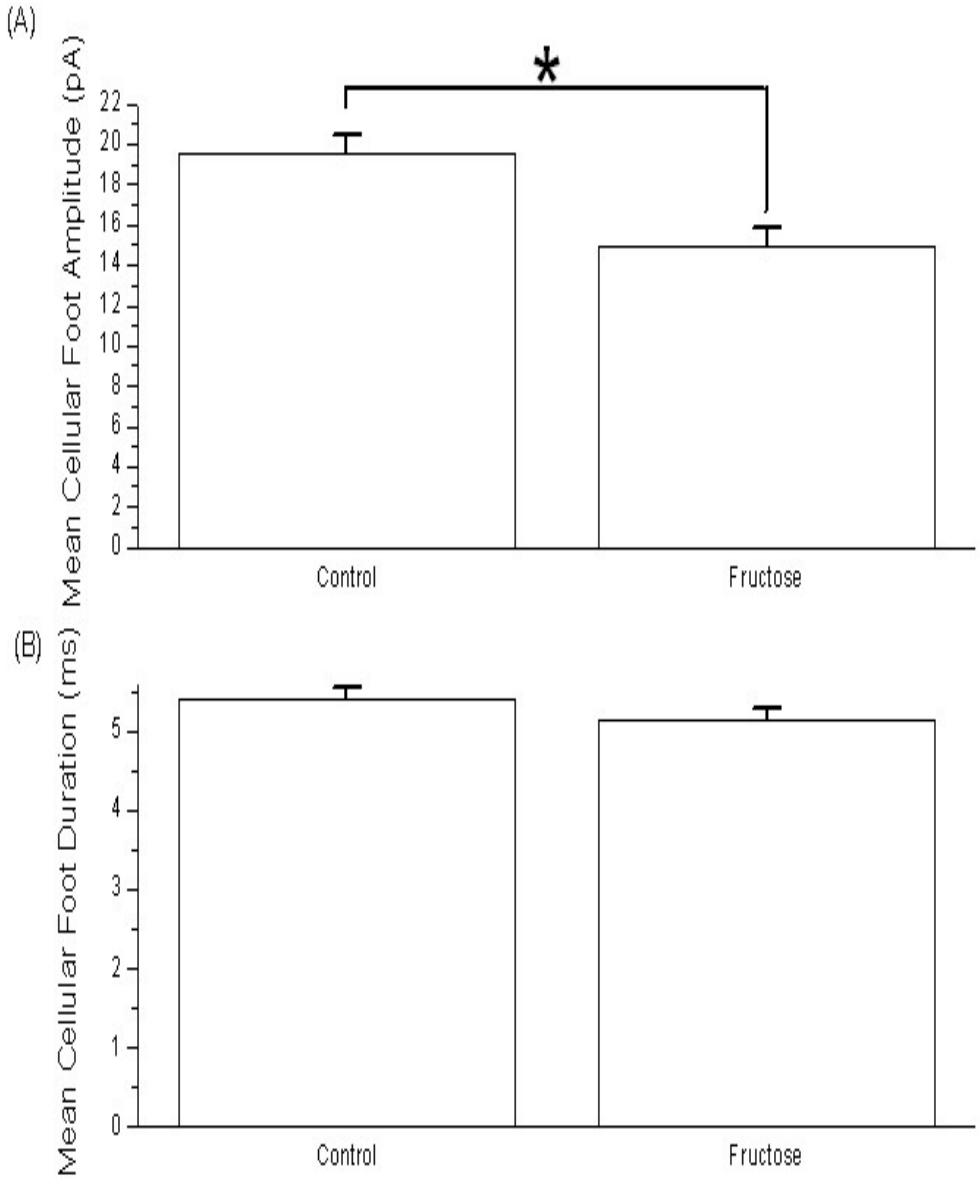

The mean cellular foot amplitude (A) and the mean cellular foot duration (B). N= 88 cells from five rats for the controls and 68 cells from four fructose-fed rats.

Figure 21:

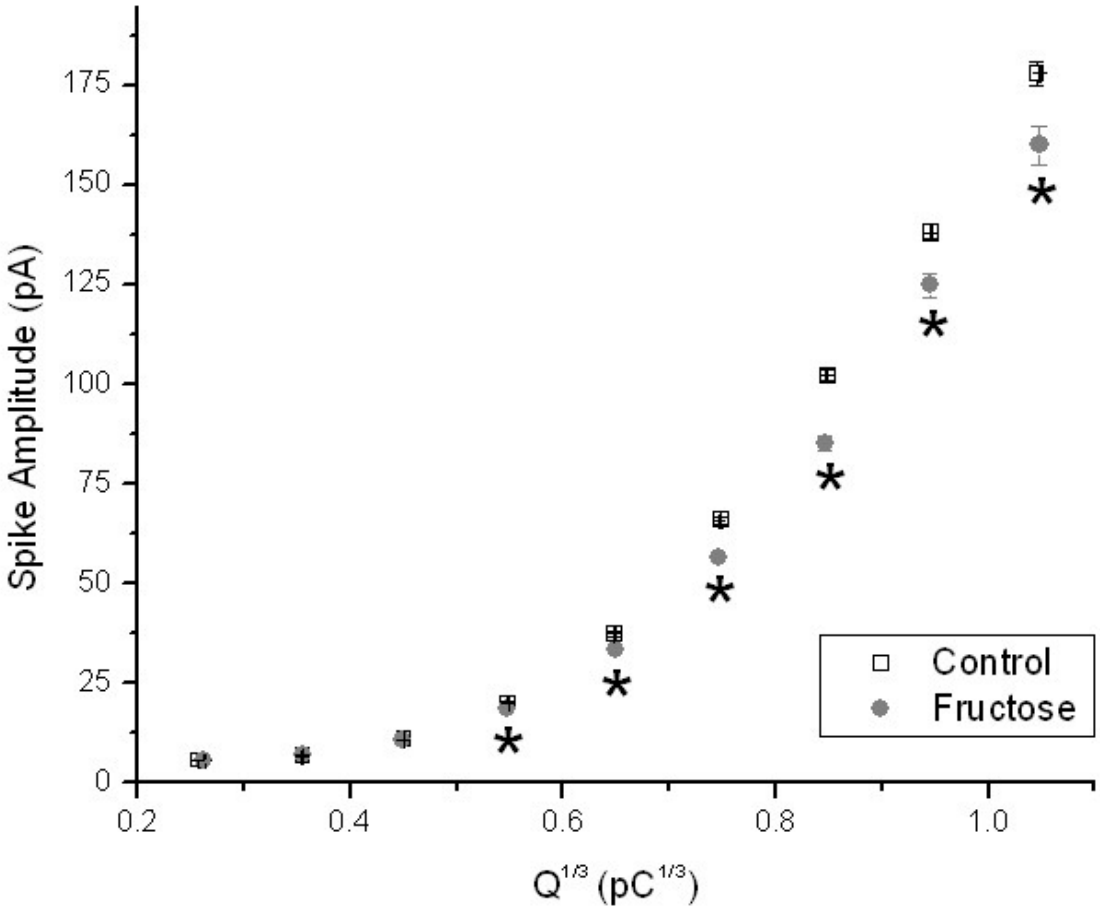

The spike amplitude at matched bin size of 0.1 $pC^{1/3}$. Bins with less than 400 events were excluded. N= 26434 events for the controls and 16151 events for the fructose-fed rats.

Figure 22:

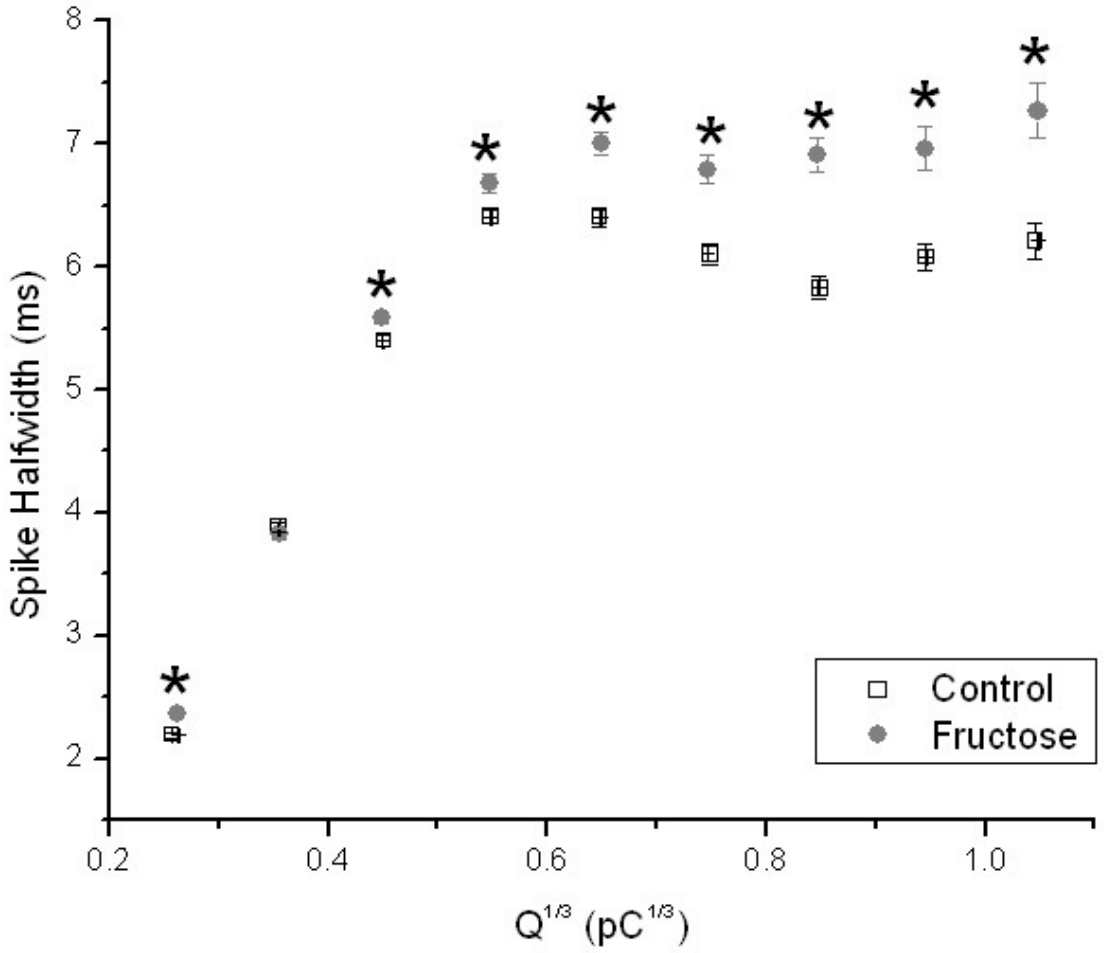

The spike half width at matched bin size of 0.1 $pC^{1/3}$. Bins with less than 400 events were excluded. N= 26434 events for the controls and 16151 events for the fructose-fed rats.

Figure 23:

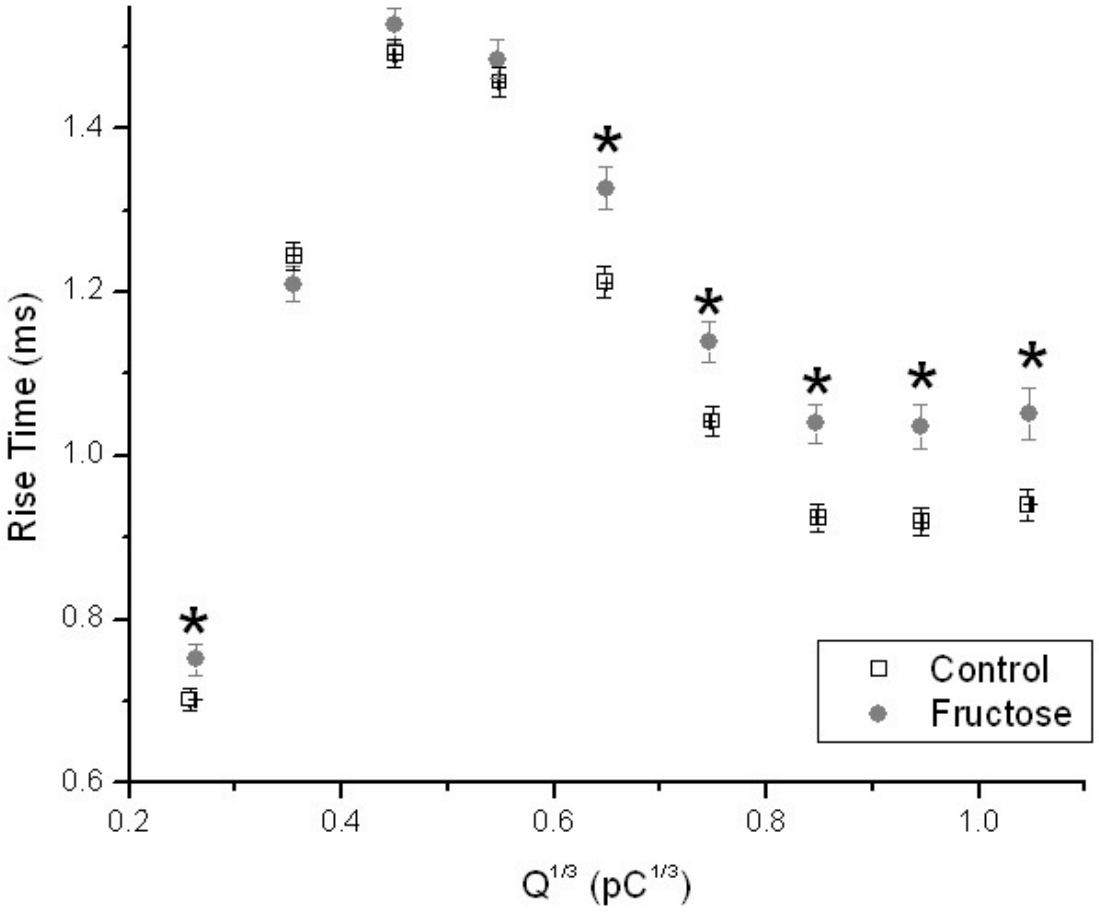

The 50-90% rise time at matched bin size of 0.1 $pC^{1/3}$. Bins with less than 400 events were excluded. N= 26434 events for the controls and 16151 events for the fructose-fed rats.

Figure 24:

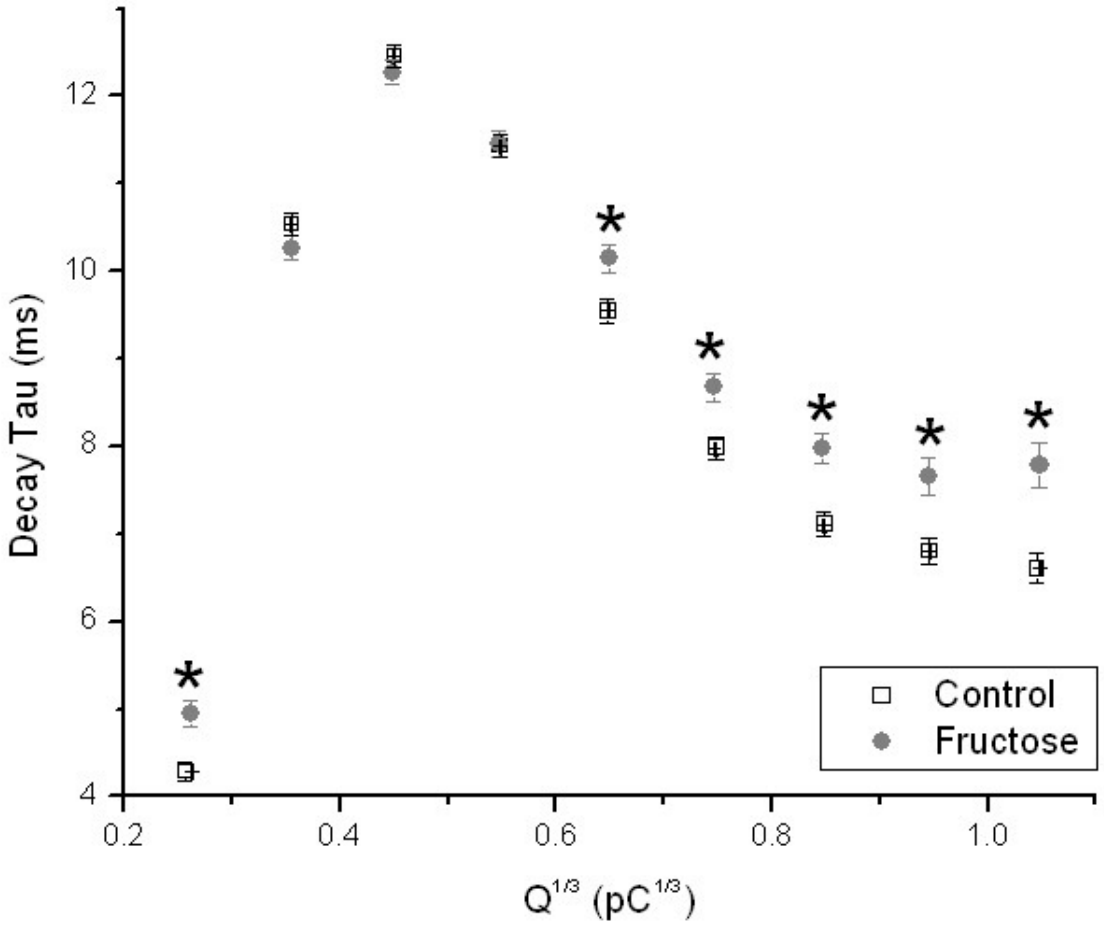

The decay time constant τ at matched bin size of 0.1 $pC^{1/3}$. Bins with less than 400 events were excluded. N= 26434 events for the controls and 16151 events for the fructose-fed rats.

Figure 25:

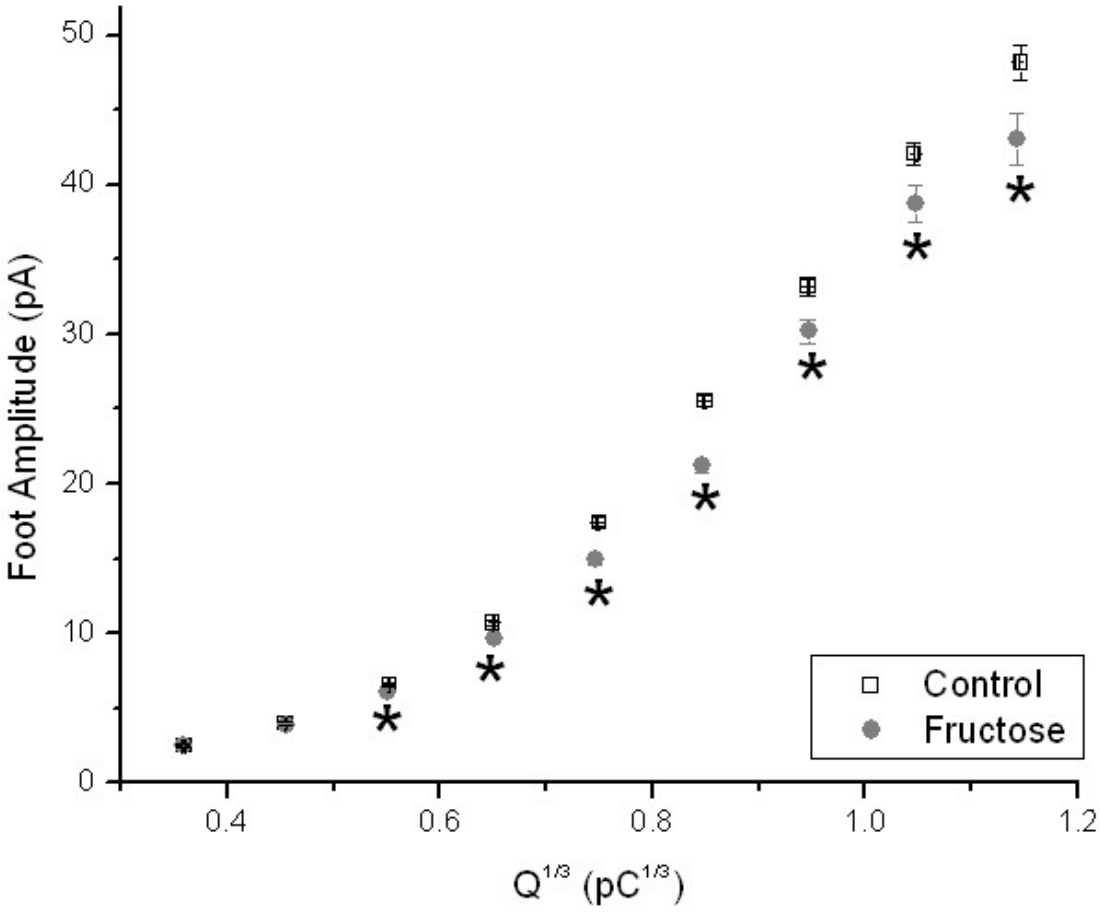

The foot amplitude at matched bin size of 0.1 $pC^{1/3}$. Bins with less than 300 events were excluded. N= 14333 events for the controls and 8395 events for the fructose-fed rats.

Figure 26:

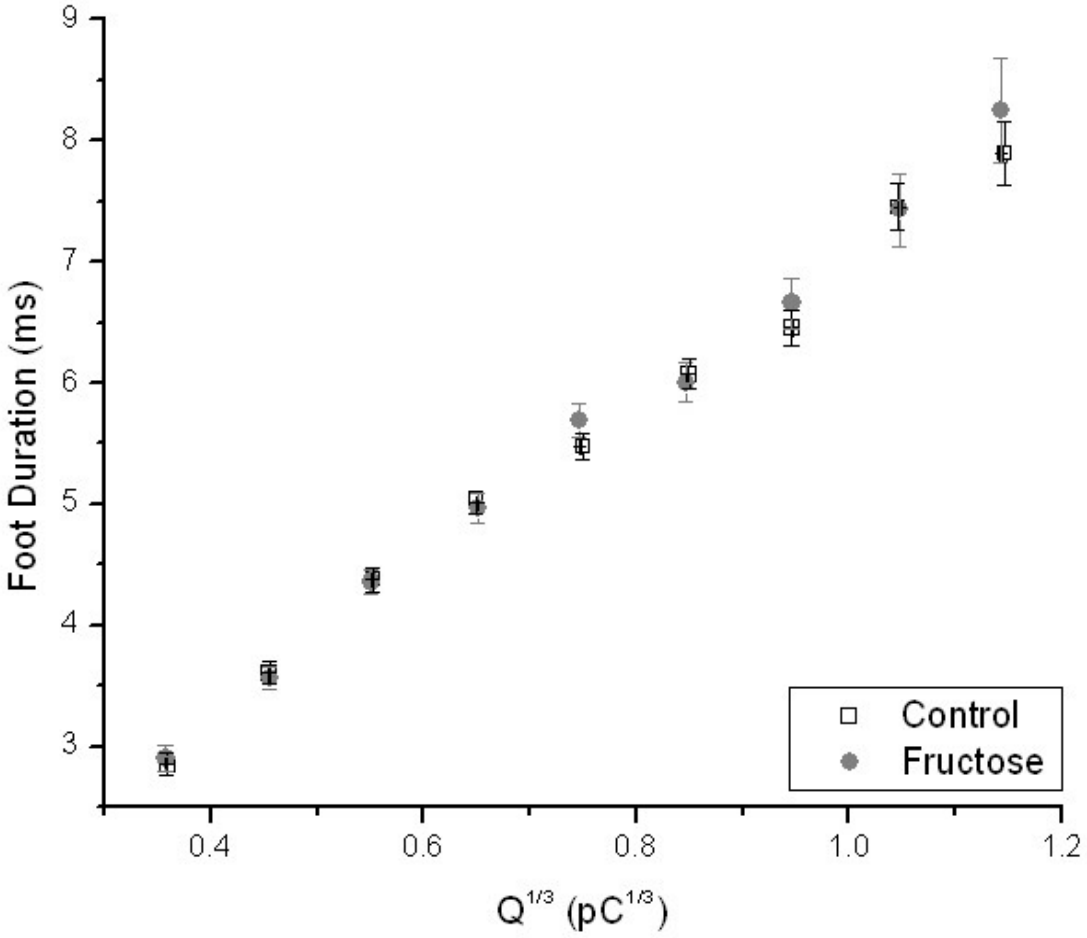

The foot duration at matched bin size of 0.1 $pC^{1/3}$. Bins with less than 300 events were excluded. N= 14333 events for the controls and 8395 events for the fructose-fed rats.

Reference List:

Elhamdani A, Zhou Z, & Artalejo CR (1998). Timing of dense-core vesicle exocytosis depends on the facilitation L-type Ca channel in adrenal chromaffin cells. *J Neurosci* **18**, 6230-6240.

Paredes RM, Etzler JC, Watts LT, Zheng W, & Lechleiter JD (2008). Chemical calcium indicators. *Methods* **46**, 143-151.

Tang KS, Tse A, & Tse FW (2005). Differential regulation of multiple populations of granules in rat adrenal chromaffin cells by culture duration and cyclic AMP. *J Neurochem* **92**, 1126-1139.

Tang KS, Wang N, Tse A, & Tse FW (2007). Influence of quantal size and cAMP on the kinetics of quantal catecholamine release from rat chromaffin cells. *Biophys J* **92**, 2735-2746.

Xu J, Tang KS, Lu VB, Weerasinghe CP, Tse A, & Tse FW (2005). Maintenance of quantal size and immediately releasable granules in rat chromaffin cells by glucocorticoid. *Am J Physiol Cell Physiol* **289**, C1122-C1133.

Chapter 4 Discussion:

When stimulated with carbachol, a nonselective cholinergic agonist, the chromaffin cells from the fructose-fed rats released ~2.4-fold the amount of catecholamine in 3 minutes in comparison with control cells (which was estimated from the time integral of the amperometric signal; Fig. 2A in Chapter 3). The individual granules from the fructose-fed rat chromaffin cells also secrete ~1.4-fold catecholamine in comparison with those in control cells (i.e. have a larger value of Q; Fig. 2B in Chapter 3), which partly accounts for the increase in overall catecholamine secretion. This increase in Q was not due to a higher cellular content of catecholamine or a larger rise in $[Ca^{2+}]_I$ (Figs. 5 and 6 in Chapter 3). Although fructose feeding did not significantly change the mean number of individual amperometric events that were detected during the entire 3 minute recording, an interesting pattern emerged when I compared the number of amperometric signals recorded during the 30s of carbachol application with that recorded during the next 2.5 minutes. During the 30s of carbachol application, fructose feeding reduced the mean number of amperometric events by 37% (35.72±3.70 events in the control cells vs. 22.39±2.51 events in the cells from fructose-fed rats; Fig. 1A). In contrast, for the 2.5 mins after the application of carbachol, ~37% more amperometric events were detected from chromaffin cells isolated from the fructose-fed rats (59.96±7.96 events in the control cells vs. 82.27±8.65 events in the cells from fructose-fed rats; Fig. 1B). This suggests that although the control chromaffin cells had more events of catecholamine release while the cell was stimulated by carbachol, the chromaffin cells from fructose-fed rats had more events of catecholamine release after the carbachol application. The mean time integral of the amperometric trace during 30s of carbachol application was not significantly different between the control chomaffin cells and the chromaffin cells isolated from fructose-fed rats (Fig. 1C). This indicates that there was

no significant difference in the amount of catecholamine released during this time period. It is probable that the increase in the quantal size in chromaffin cells of fructose-fed rats compensated for the decrease in the mean number of amperometric events from these cells. In contrast, the time integral of the amperometric trace during the 2.5 min after the application of carbachol to fructose fed cells was 346% that of control cells (70.77±16.20pC in the control chromaffin cells vs. 244.89±61.62pC in the chromaffin cells from fructose-fed rats; Fig. 1D). This phenomenon is expected since chromaffin cells from fructose-fed rats had a larger mean cellular value for Q as well as for the number of detectable amperometric events.

There is evidence that rat adrenal chromaffin cells express M3 and M4 muscarinic acetylcholine receptors (mAChRs) (Barbara *et al.*, 1998). Rat adrenal chromaffin cells also express erg channels, which are a type of rectifying potassium channels; when these channels are inhibited in chromaffin cells the cells become more excitable (Gullo *et al.*, 2003). Hirdes *et. al.* (2004) found that when a tsA cell (with little endogenous current) was transfected with erg1 and either the mAChRs M1 or M3, stimulation of the muscarinic receptors inhibited the erg current (most likely by depleting phosphatidylinositol4,5-bisphosphate (PIP_2) at the plasma membrane) (Hirdes *et al.*, 2004). Acetylcholine (or carbachol) activates both nicotinic and muscarinic receptors on the adrenal chromaffin cells; therefore, mAChR stimulation may inhibit the erg current, which would then make the cell more excitable (Barbara *et al.*, 1998;Zaika *et al.*, 2004). If there is an increase in the muscarinic response in the fructose-fed rat chromaffin cells this could be a mechanism behind the increase in the number of events seen during the wash phase of the amperometric recording. Figure 2 shows that rat chromaffin cells indeed express mAChRs significantly since 1mM carbachol still elicited a rise in the internal calcium concentration when the chromaffin cells were bathed in an extracellular solution that had no added Ca^{2+} but with

1mM EGTA (Fig. 2). An increase in muscarinic activation can alter LDCG release through the activation of second messengers as a result of stimulating mAChRs. ATP and other molecules such as μ-opioids which are released from the LDCGs of adrenal chromaffin cells can cause feedback inhibition of LDCG release. In the case of ATP this effect is mediated via the P2Y receptor which is a G-protein coupled receptor which is coupled to $G_{i/o}$ (Chen *et al.*, 2005). Activation of $G_{i/o}$ produces $G_{\beta\gamma}$ which has been shown to be important in promoting "kiss-and-run" exocytosis (where LDCGs fuse to the plasma membrane transiently and there is incomplete release of LDCG content) which results in a decrease in the quantal size of amperometric events and less overall catecholamine release (Chen *et al.*, 2005). This effect of $G_{\beta\gamma}$ can be abolished by stimulating the muscarinic receptors, that are coupled via a G_q pathway, which in turn activates protein kinase C (PKC) to increase the quantal size and overall catecholamine release (Chen *et al.*, 2005). The above muscarinic effect may contribute to the larger quantal size seen in the chromaffin cells of fructose-fed rats (Chen *et al.*, 2005). The mAChR M3 receptors activate G_q and PKC whereas M4 activates $G_{i/o}$, therefore the ratio of active mACh M3 to M4 receptors could have a significant impact on the quantal size of amperometric events when cells are stimulated with a cholinergic agonist (Barbara *et al.*, 1998).

Figure 3 summarized the kinetic changes associated with fructose feeding which were detected when the cells were stimulated with carbachol. When the events from each group of chromaffin cells are compared at intermediate ranges of $Q^{1/3}$ they are faster and taller in the chromaffin cells from the fructose-fed rats. The decrease in half width found in the events from the chromaffin cells of fructose-fed rats is due to both a faster rising phase and decay phase of the event. The events which contain a foot have a foot with a larger amplitude and shorter duration in the events at intermediate ranges of $Q^{1/3}$ from the chromaffin cells of fructose-fed

rats. A taller foot with a shorter duration could be caused by a larger fusion pore or a granule matrix that undergoes more rapid dissolution (Amatore *et al.*, 2007). Both a larger fusion pore and granule matrix undergoing more rapid dissolution could also cause changes in the spike kinetics which are seen in the results (Amatore *et al.*, 2007;Wang *et al.*, 2010). A larger fusion pore could be due to an altered granule and/or plasma membrane lipid composition (Amatore *et al.*, 2007;Wang *et al.*, 2010). For example, overloading a cell with cholesterol causes a more stable fusion pore with a foot signal that is taller and lasts longer, while depleting cholesterol from the plasma membrane results in a fusion pore which is less stable, resulting in a foot signal which is shorter in both amplitude and duration (Wang *et al.*, 2010). A granule matrix that undergoes more rapid dissolution may be caused by a change in the expression of the granule matrix proteins. For example knocking out the granule packaging proteins, chromogranins, not only reduced the quantal size of individual granules but also affected the kinetics of granule release (Montesinos *et al.*, 2008;Diaz-Vera *et al.*, 2010). Chromogranin A knockouts had faster kinetics of release, whereas chromogranin B knockouts had slower kinetics of release (Montesinos *et al.*, 2008;Diaz-Vera *et al.*, 2010).

There is a large discrepancy between the amperometric results obtained from stimulating the chromaffin cells with carbachol and stimulating with 50mM KCl. When cells are stimulated with high K^+ the mean cellular quantal size and the mean number of events per recording are decreased in the chromaffin cells from fructose-fed rats. These two effects indicate a decrease in the total amount of catecholamine released from the chromaffin cells of fructose-fed rats. However, the mean time integrals of the total amperometric traces are unchanged between the control and fructose-fed chromaffin cells which confuses the issue of whether or not there is less catecholamine secretion from the chromaffin cells of the fructose-fed rats. This discrepancy can

arise from the higher frequency of events seen when cells are stimulated with the high K^+. When amperometric events occur at very close intervals it becomes impossible to distinguish them for analysis. Chromaffin cells stimulated with high K^+ have a higher (~2 fold) mean number of events (even when comparing only the first three minutes of the recording to match the time course of the carbachol application) and a higher mean cellular quantal size (~1.4 fold, see Table 1). The half width at matched $Q^{1/3}$ (in the range of $0.3pC^{1/3}$ to $0.8pC^{1/3}$) is faster in the control cells stimulated with high K^+ then carbachol, which also indicates the application of high K^+ stimulates the chromaffin cells more strongly than the carbachol application (Fig. 4). The discrepancies between the findings when cells were stimulated with carbachol and when they were stimulated with high K^+ could be partially due to the stronger stimulation with the K^+ application triggering other pools of releasable granules (see below). The stronger stimulation seen from high K^+ application could also distort differences in other kinetic parameters of the amperometric signals between control chromaffin cells and chromaffin cells from fructose-fed rats (Grabner *et al.*, 2005).

It has been shown previously that the distribution of Q for a large number of amperometric events can be better described as the summation two to three Gaussian curves (Grabner *et al.*, 2005;Tang *et al.*, 2005). The different population of granules identified in such analysis could be the result of different modes of exocytosis (i.e. "kiss-and-run" vs. full fusion) and/or the result of secretion from different pools of exocytosis (van Kempen *et al.*, 2011;Stevens *et al.*, 2011). When I fit 2 Gaussian curves to the histograms of the distribution of Q for the control cells stimulated with high K^+ and carbachol, I found that the two methods of stimulation did not trigger the same proportion of large $Q^{1/3}$ events (modal $Q^{1/3}$ ~$0.9pC^{1/3}$, 56.89% vs.39.41% of the total area respectively) and the small $Q^{1/3}$ events (modal $Q^{1/3}$~$0.5pC^{1/3}$,

43.42% of the total area and 60.59% of the total area respectively) (Fig. 5). Interestingly the dominant effect of fructose feeding on the kinetics of individual amperometric spikes was not only in opposite directions for the two methods of stimulation, but seem to involve different populations of LDCGs. The signals from the fructose-fed rat cells stimulated with carbachol were faster and taller at ranges of $Q^{1/3}$ from 0.3-0.7$pC^{1/3}$ (the small $Q^{1/3}$ population, see Chapter 3 Figs. 9-13) while the signals from the fructose-fed rats stimulated with high K^+ were slower and shorter at ranges of $Q^{1/3}$ over 0.6$pC^{1/3}$ (the large $Q^{1/3}$ population, see Chapter 3 Figs. 21-25).

I have already explained how activation of the mAChR (by carbachol) could promote more full fusion and less "kiss-and-run" release (see above) so I will focus on the potential to release a different population of granules. Classical studies employing flash photolysis of cage-Ca^{2+} have identified three pools of granules in chromaffin cells; the readily releasable pool (RRP, which are granules that are docked to the plasma membrane through a SNARE complex), the slow releasable pool (SRP, which are LDCGs that are situated close to the membrane but have not formed a snare complex and thus cannot be triggered to exocytosis as quickly), and the reserve pool (which are granules that are situated away from the plasma membrane and must be transported to the cell surface by the actin network) (Stevens *et al.*, 2011). When Ca^{2+} entry via VGCC was employed to trigger exocytosis, an immediately releasable pool (IRP, which are granules of the RRP that are situated close to the voltage gated calcium channels, VGCCs) has also been found; this pool would be able to undergo exocytosis at lower levels of VGCC activation than the RRP (Stevens *et al.*, 2011;Alvarez & Marengo, 2011). It has been shown that the IRP is not the result of random distribution of granules from the RRP but that granules of the IRP are targeted to sites of calcium entry (Alvarez & Marengo, 2011). It is possible that LDCGs in chromaffin cells from fructose-fed rats have a larger quantal size in certain IRP that can be

more selectively triggered by the weaker stimulation with carbachol; however, when the same cells are stimulated more strongly with high $[K^+]_{ext}$, release from the multiple granule pools is triggered and the release from the IRP would be obscured. Another possible reason why there is a difference between the results obtained by stimulating the chromaffin cells with carbachol and stimulating the cells with KCl is the activation of mAChRs by carbachol. Although the activation of mAChRs can contribute to the elevation of $[Ca^{2+}]_i$ in a chromaffin cell line (PC-12), the entry of extracellular Ca^{2+} as a consequence of the activation of nAChRs is the major source of the rise in $[Ca^{2+}]_i$ in PC-12 cells when they are stimulated by acetylcholine (Taylor & Peers, 2000). When nAChRs are activated, they allow the influx of sodium and calcium, which depolarizes the cell and activates voltage-gated calcium channels (VGCCs), and the influx of calcium though both the nAChRs and VGCCs trigger exocytosis (Harkins & Fox, 1998;Taylor & Peers, 2000). Application of high potassium also depolarizes the cell and opens VGCCs, but will not activate mAChRs. Stimulation of the Gq coupled mAChRs causes the release of Ca^{2+} from inositol-3-phosphate (IP_3)-sensitive calcium stores inside the cell, and the depletion of such stores will in turn activate capacitative calcium entry into the cell (Guo *et al.*, 1996;Barbara *et al.*, 1998;Taylor & Peers, 2000). The chromaffin cells from fructose-fed rats could have a larger muscarinic response than the chromaffin cells from the control rats; this in turn could lead to an increase in exocytosis of different populations of granules. If certain triggered populations of granules turn out to have a larger Q, it will also contribute to make the mean cellular Q larger (Grabner *et al.*, 2005;Tang *et al.*, 2005). Another pool of granules which may be preferentially triggered by stimulation with carbachol but not with high K^+ is the highly calcium-sensitive pool (HCSP), which may be selectively triggered by the release of internal calcium stores (Stevens *et al.*, 2011;Yang *et al.*, 2007). If the LDCGs in the HCSP of chromaffin cells have a larger Q, then an

increase in muscarinic stimulation could increase the mean cellular Q either directly through the triggered release of internal calcium stores or indirectly as PKC promotes an increase in the size of the HCSP (Yang *et al.*, 2007). Fructose feeding might also cause a shift in the source of Ca^{2+} entry/release with the activation of mAChRs in chromaffin cells, because chromaffin cells from fructose-fed tend to have a smaller rise in $[Ca^{2+}]_i$ for the entire duration after carbachol stimulation yet stimulated more than twice the amount of catecholamine release (Fig. 2). It is possible that the chromaffin cells from fructose-fed rats have a population of LDCGs with a larger Q in the HCSP. There may also be a population of granules which is close to sites of capacitative calcium entry. In bovine chromaffin cells capacitative calcium entry is triggered by the depletion of internal calcium stores and the resultant calcium entry can trigger exocytosis (Zerbes *et al.*, 2001;Fomina & Nowycky, 1999). If the Q of the granules that are activated by these stores is larger in the chromaffin cells from fructose-fed rats then this could be the mechanism underlying the difference between stimulation with high K^+ and carbachol.

In summary, when chromaffin cells from fructose-fed rats are stimulated with carbachol, to mimic a more physiological stimulus, they secrete more catecholamine than chromaffin cells from control rats. This increase in catecholamine secretion could be a factor in the development of hypertension that is seen in the fructose-fed rats. A possible cause of the increase in catecholamine secretion is production of more second messengers from a G_q pathway and less activation of the $G_{i/o}$ pathway, resulting in a decrease in "kiss-and-run" kinetics and more full fusion of LDCGs, hence leading to more quantal catecholamine release even from individual granules. Another possibility is that chromaffin cells from the fructose-fed rats could have a larger population of granules which in the IRP and/or HSCP would only be apparent when stimulating acetylcholine receptors. Determining the mechanism which causes an increase in

catecholamine release from the fructose-fed rat when cells are stimulated is important for future research and may lead to therapeutic targets to try to combat hypertension caused by fructose feeding. The results shown in this thesis indicate that a high fructose diet may cause a higher release of catecholamine from the adrenal chromaffin cells, which may contribute to hypertension; it may then be advisable to limit fructose consumption in order to avoid these negative health consequences.

Tables:

Table 1: Comparison of control and fructose-fed rat chromaffin cells stimulated with either 50mM $[K^+]_{ext}$ or 1mM carbachol.

Condition	Mean Cellular Q (pC)	Mean Number of Events after 3min of recording	Number of cells sampled
Control stimulated with KCl	0.402±0.018	217.66±11.92	88
Control stimulated with carbachol	0.278±0.019*	95.68±9.29**	47
Fructose stimulated with KCl	0.327±0.020	184.24±11.91	68
Fructose stimulated with carbachol	0.381±0.022	104.66±8.75ǂ	44

*$p<5X10^{-5}$ compared with the control chromaffin cells stimulated with KCl

**$p<1X10^{-5}$ compared with the control chromaffin cells stimulated with KCl

ǂ$p<1X10^{-5}$ compared with the chromaffin cells from fructose-fed rats stimulated with KCl

Figures:

Figure 1:

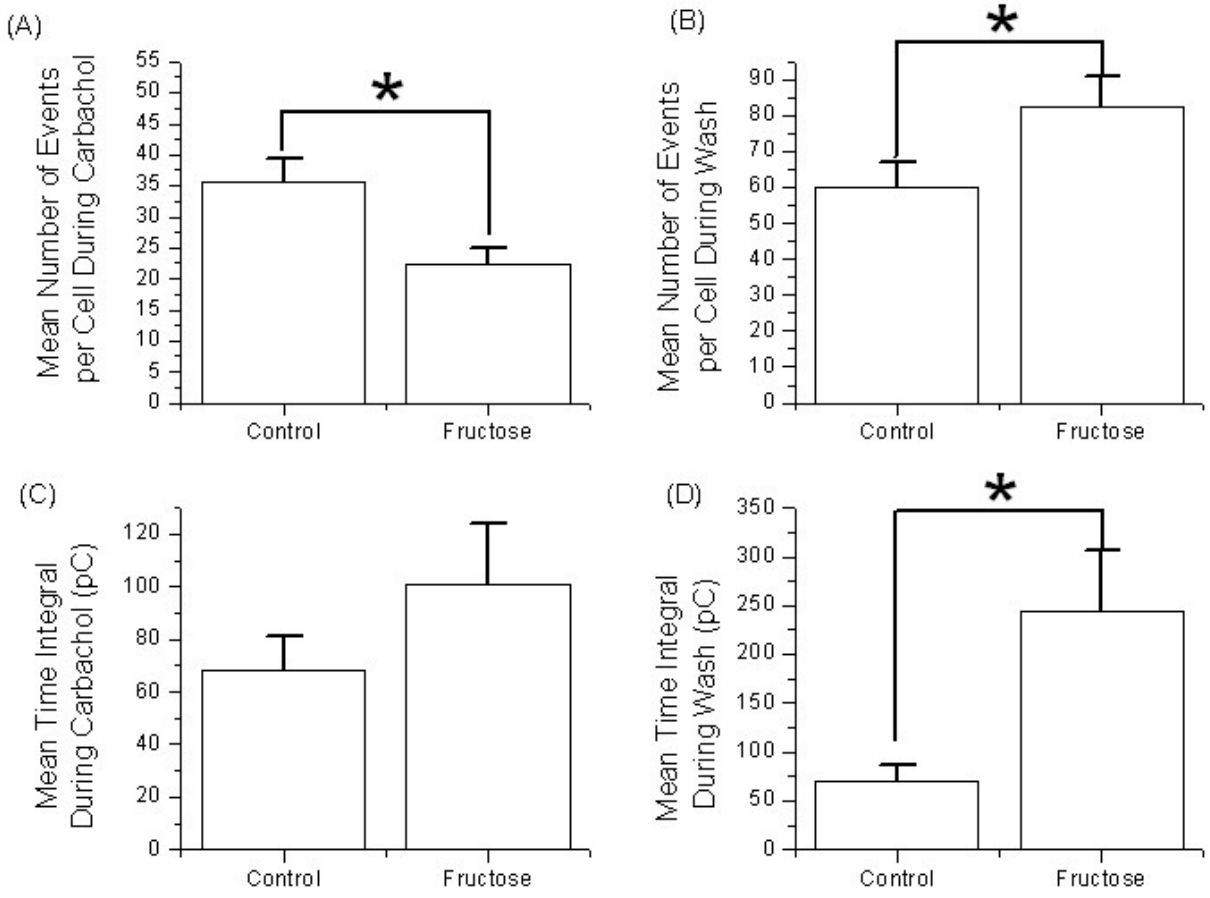

The mean number of events while carbachol is applied (A). The mean number of events during the remainder of the recording after carbachol is washed out (B). The mean time integral of the amperometric trace while carbachol is applied (C). The mean time integral of the amperometric trace during the remainder of the recording after carbachol is washed out (D). For the mean number of events N=47 cells for the control chromaffin cells and N=44 cells for the chromaffin cells from fructose-fed rats. For the mean time integral N=27 cells for the control chromaffin cells and N=26 for the chromaffin cells from fructose-fed rats.

Figure 2:

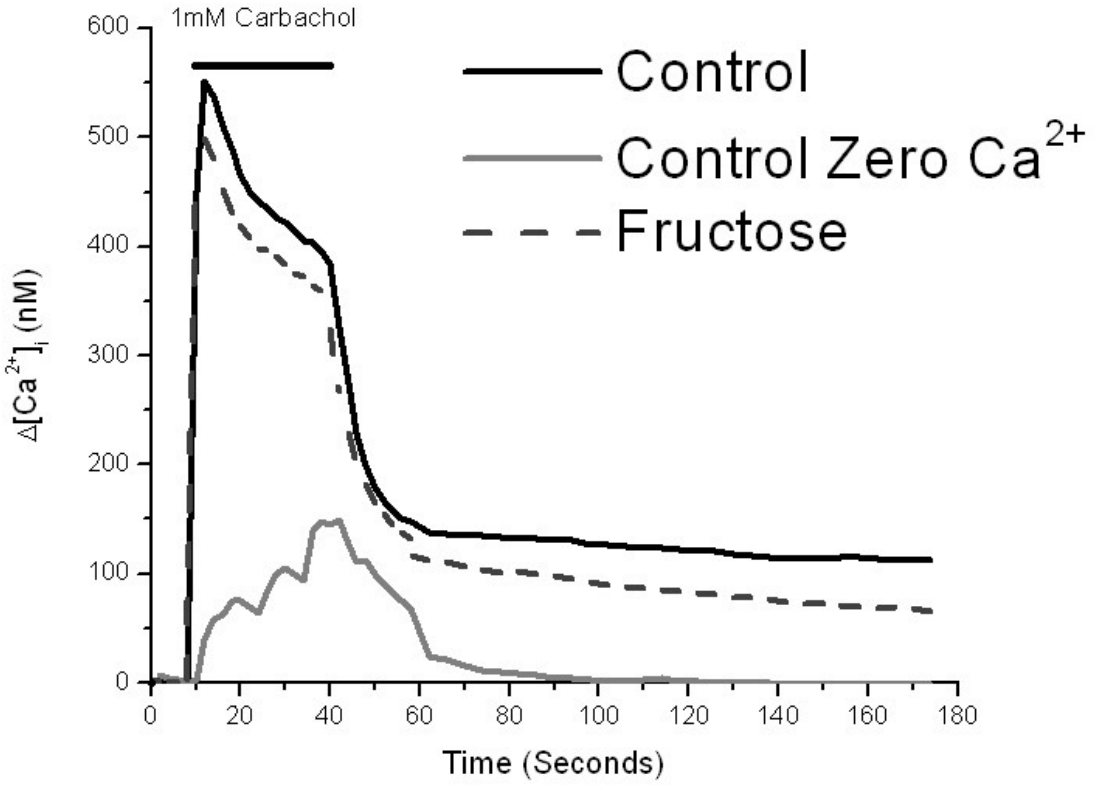

The change in the cytosolic calcium concentration when cells are stimulated with 1mM carbachol in either 2mM extracellular calcium or 0mM extra cellular calcium. N=50 cells for the control and 46 cells for the chromaffin cells from fructose-fed rats. N=31 cells for the control cells stimulated with zero extracellular calcium.

Figure 3:

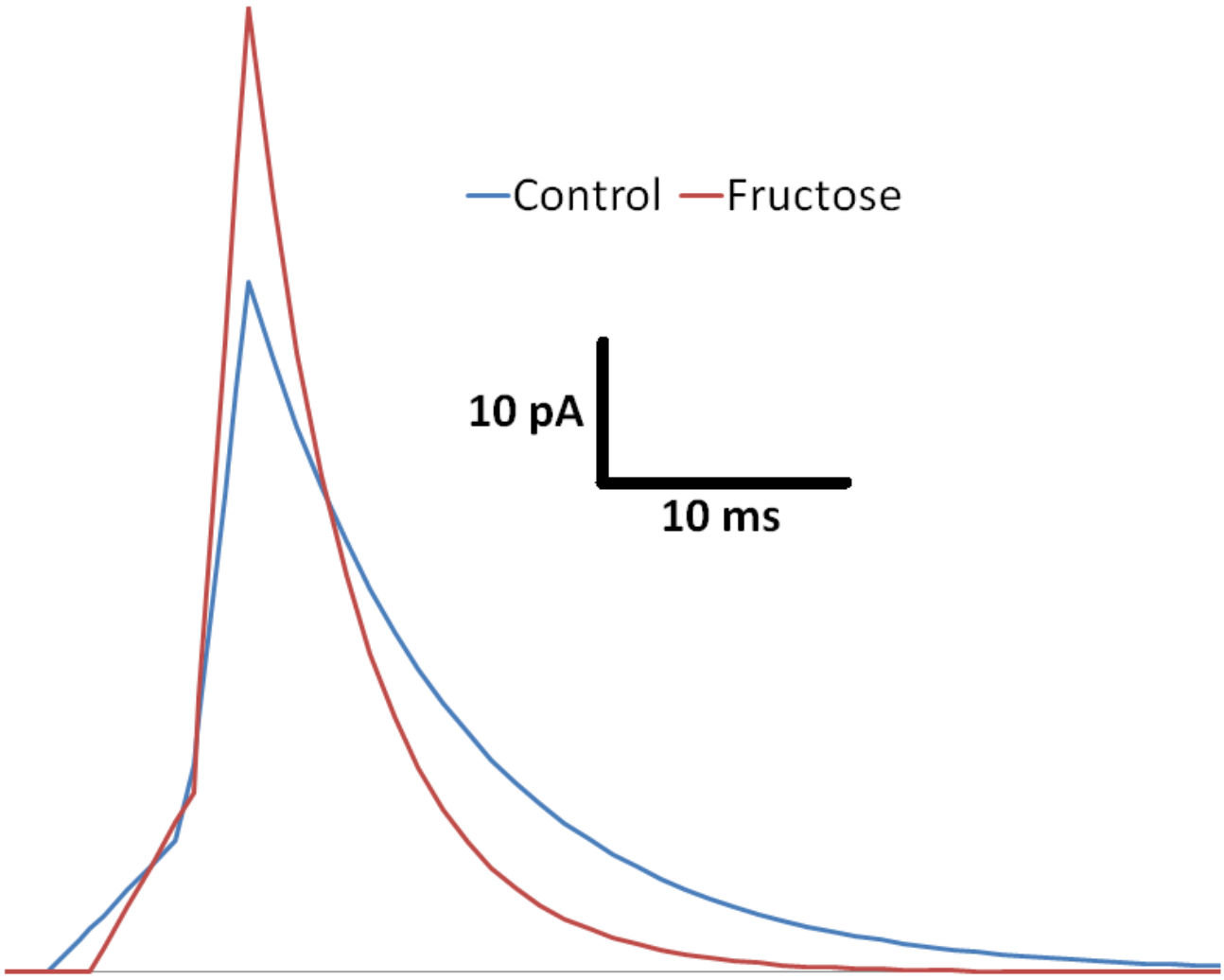

A summary of the changes in the kinetics of granule release at matched quantal size based on mean values between 0.6-0.7pC$^{1/3}$

Figure 4:

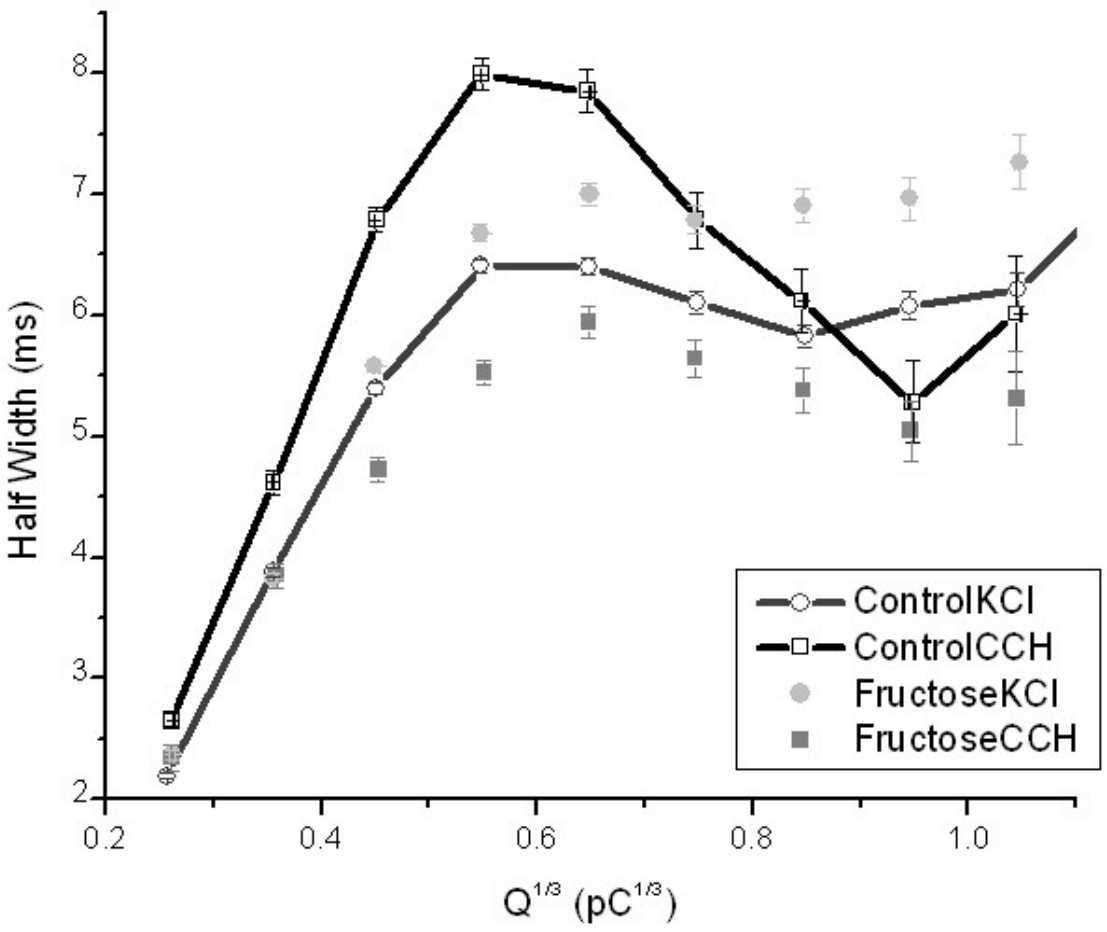

The spike half width at matched bin size of 0.1 $pC^{1/3}$. For chromaffin cells stimulated with carbachol N= 4497 events for the controls and 4605 events for the fructose-fed rats. For chromaffin cells stimulated with 50mM $[K^+]_{ext}$ N= 26434 events for the controls and 16151 events for the fructose-fed rats.

Figure 5:

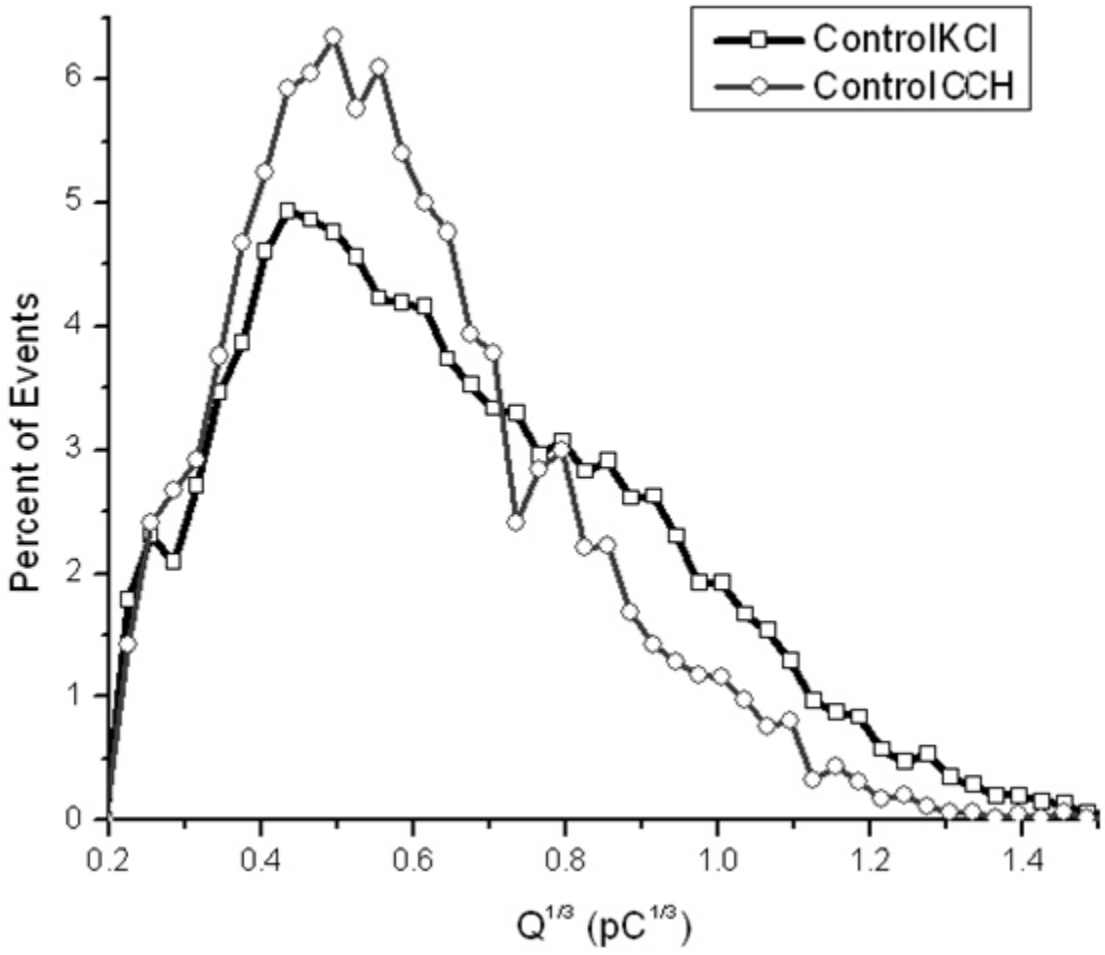

Histograms of control chromaffin cells stimulated with either 50mM KCl or 1mM carbachol, N=26434 events and 4497 events respectively.

Reference List:

Alvarez YD & Marengo FD (2011). The immediately releasable vesicle pool: highly coupled secretion in chromaffin and other neuroendocrine cells. *J Neurochem* **116**, 155-163.

Amatore C, Arbault S, Bonifas I, Guille M, Lemaitre F, & Verchier Y (2007). Relationship between amperometric pre-spike feet and secretion granule composition in chromaffin cells: an overview. *Biophys Chem* **129**, 181-189.

Barbara JG, Lemos VS, & Takeda K (1998). Pre- and post-synaptic muscarinic receptors in thin slices of rat adrenal gland. *Eur J Neurosci* **10**, 3535-3545.

Chen XK, Wang LC, Zhou Y, Cai Q, Prakriya M, Duan KL, Sheng ZH, Lingle C, & Zhou Z (2005). Activation of GPCRs modulates quantal size in chromaffin cells through G(betagamma) and PKC. *Nat Neurosci* **8**, 1160-1168.

Diaz-Vera J, Morales YG, Hernandez-Fernaud JR, Camacho M, Montesinos MS, Calegari F, Huttner WB, Borges R, & Machado JD (2010). Chromogranin B gene ablation reduces the catecholamine cargo and decelerates exocytosis in chromaffin secretory vesicles. *J Neurosci* **30**, 950-957.

Fomina AF & Nowycky MC (1999). A current activated on depletion of intracellular Ca2+ stores can regulate exocytosis in adrenal chromaffin cells. *J Neurosci* **19**, 3711-3722.

Grabner CP, Price SD, Lysakowski A, & Fox AP (2005). Mouse chromaffin cells have two populations of dense core vesicles. *J Neurophysiol* **94**, 2093-2104.

Gullo F, Ales E, Rosati B, Lecchi M, Masi A, Guasti L, Cano-Abad MF, Arcangeli A, Lopez MG, & Wanke E (2003). ERG K+ channel blockade enhances firing and epinephrine secretion in rat chromaffin cells: the missing link to LQT2-related sudden death? *FASEB J* **17**, 330-332.

Guo X, Przywara DA, Wakade TD, & Wakade AR (1996). Exocytosis coupled to mobilization of intracellular calcium by muscarine and caffeine in rat chromaffin cells. *J Neurochem* **67**, 155-162.

Harkins AB & Fox AP (1998). Activation of nicotinic acetylcholine receptors augments calcium channel-mediated exocytosis in rat pheochromocytoma (PC12) cells. *J Gen Physiol* **111**, 257-269.

Hirdes W, Horowitz LF, & Hille B (2004). Muscarinic modulation of erg potassium current. *J Physiol* **559**, 67-84.

Montesinos MS, Machado JD, Camacho M, Diaz J, Morales YG, Alvarez dlR, Carmona E, Castaneyra A, Viveros OH, O'Connor DT, Mahata SK, & Borges R (2008). The crucial role of

chromogranins in storage and exocytosis revealed using chromaffin cells from chromogranin A null mouse. *J Neurosci* **28**, 3350-3358.

Stevens DR, Schirra C, Becherer U, & Rettig J (2011). Vesicle pools: lessons from adrenal chromaffin cells. *Front Synaptic Neurosci* **3**, 2.

Tang KS, Tse A, & Tse FW (2005). Differential regulation of multiple populations of granules in rat adrenal chromaffin cells by culture duration and cyclic AMP. *J Neurochem* **92**, 1126-1139.

Taylor SC & Peers C (2000). Three distinct Ca(2+) influx pathways couple acetylcholine receptor activation to catecholamine secretion from PC12 cells. *J Neurochem* **75**, 1583-1589.

van Kempen GT, vanderLeest HT, van den Berg RJ, Eilers P, & Westerink RH (2011). Three distinct modes of exocytosis revealed by amperometry in neuroendocrine cells. *Biophys J* **100**, 968-977.

Wang N, Kwan C, Gong X, de Chaves EP, Tse A, & Tse FW (2010). Influence of cholesterol on catecholamine release from the fusion pore of large dense core chromaffin granules. *J Neurosci* **30**, 3904-3911.

Yang Y, Craig TJ, Chen X, Ciufo LF, Takahashi M, Morgan A, & Gillis KD (2007). Phosphomimetic mutation of Ser-187 of SNAP-25 increases both syntaxin binding and highly Ca^{2+}-sensitive exocytosis. *J Gen Physiol* **129**, 233-244.

Zaika OL, Pochynyuk OM, Kostyuk PG, Yavorskaya EN, & Lukyanetz EA (2004). Acetylcholine-induced calcium signalling in adrenaline- and noradrenaline-containing adrenal chromaffin cells. *Arch Biochem Biophys* **424**, 23-32.

Zerbes M, Clark CL, & Powis DA (2001). Neurotransmitter release from bovine adrenal chromaffin cells is modulated by capacitative Ca^{2+} entry driven by depleted internal Ca^{2+} stores. *Cell Calcium* **29**, 49-58.

Appendix:

The Nile Rat, a model of diabetes

This chapter covers the few experiments on Nile rats (*Arvicanthis niloticus)* which were in too limited supply (a few animals every 12 months) for a complete study.

The Nile rat is a wild African grass rat which develops diabetes and other symptoms of metabolic syndrome, such as high plasma triglyceride levels (Noda *et al.* 2010) in captivity. By the time the Nile rats reach one year of age, while being kept in captivity and fed the chow of laboratory rats, around 90% of the males have developed diabetes (Noda *et al*. 2010). The diabetic Nile rats have an elevated blood pressure in comparison to non-diabetic Nile rats, but only at ages less than 10 months old (Noda *et al*. 2010). My collaborator, Dr. Yves Sauve (Department of Physiology, University of Alberta), raised a colony of Nile rats in Edmonton. For my experiments I employed carbon fibre amperometry to examine the adrenal chromaffin cells isolated from four 1 year old Nile rats that had been fed the standard chow of laboratory rats since weaning. One of these Nile rats had a blood glucose of 4.9mM, and is considered the control (normal) animal; another Nile rat had a blood glucose of 7.1mM and it will be referred to here as borderline diabetic: two other Nile rats had blood glucose levels of 14.4mM and 22.3mM, respectively and they are considered to be diabetic. Blood pressure was not measured from any of the above animals, so it is unknown if the borderline or diabetic Nile rats were hypertensive. A comparison of the mean cellular quantal size between each class of animals showed no significant difference (Fig. 1A), nor was there any change in the mean number of events recorded from individual cells stimulated for 5 minuites by perfusing the bath with a solution containing elevated (50 mM) K^+ (Fig. 1B). When I compared the distribution of the $Q^{1/3}$

of all the amperometric events for each class of animals there is no obvious difference between the cells from the borderline diabetic Nile rat and those from the control Nile rat (fig. 2), and the Kolmolgrov-Smirnov (K-S) test on the cumulative distributions had a p=0.0563 indicating that these two curves are not significantly different at the 0.05 level of significance (data not shown). In contrast, the distribution of events from the diabetic Nile rats had a much larger proportion of amperometric events with very small values of $Q^{1/3}$ which makes the distribution obviously bimodal. When the cumulative distribution of $Q^{1/3}$ from the diabetic Nile rats was compared with that of the either of the other 2 classes of animals with a K-S test the p value was $<10^{-4}$, indicating that there was significant difference in the distribution of $Q^{1/3}$. The above analyses suggest that although there was no significant change in mean cellular quantal size for the chromaffin cells from diabetic Nile rats, these animals might have a population of granules that individually released a much smaller amount of catecholamine. Interestingly, when chromaffin cells isolated from fructose-fed rats were stimulated by 50 mM of K^+ they also released a larger proportion of granules with smaller values of Q (Fig. 15 in Chapter 3). Moreover, in comparison to the control animal, the amperometric spikes from the borderline diabetic Nile rat had a longer half-width at matched ranges of $Q^{1/3}$ from 0.3-1.3$pC^{1/3}$, while the amperometric spikes from the diabetic Nile rats had a longer half-width at matched ranges of $Q^{1/3}$ from 0.4-0.6$pC^{1/3}$ and 0.7-1.3$pC^{1/3}$. These patterns for both the borderline diabetic and diabetic groups are similar to the pattern observed in the fructose-fed rats stimulated with 50mM K^+ (Fig. 3). The spike amplitude for the borderline diabetic group was only smaller than the controls at some ranges of $Q^{1/3}$ (0.4-0.6$pC^{1/3}$, 0.7-0.8 $pC^{1/3}$ and 0.9-1.0 $pC^{1/3}$); this does not follow the trends found with the fructose-fed rats (Fig. 4). The spike amplitude for the diabetic group was actually larger at some lower ranges of $Q^{1/3}$ (0.4-0.6$pC^{1/3}$) but was smaller for the higher ranges of $Q^{1/3}$ (0.7-1.3$pC^{1/3}$); this

pattern of change is similar to that observed when cells from fructose-fed rats (stimulated with 50 mM K^+) were compared to control cells. In summary, when stimulated by 50 mM K^+ the amperometric signals from chromaffin cells of Nile rats that developed diabetes had patterns of variations that are similar to those in rat chromaffin cells after fructose-feeding, moreover, these patterns were less evident when the Nile rats were only borderline diabetic. There were only a few Nile rats used in this study so far because it takes a year to breed them, so I did not have access to a large number of Nile rats while conducting my research.

Figures:

Figure I:

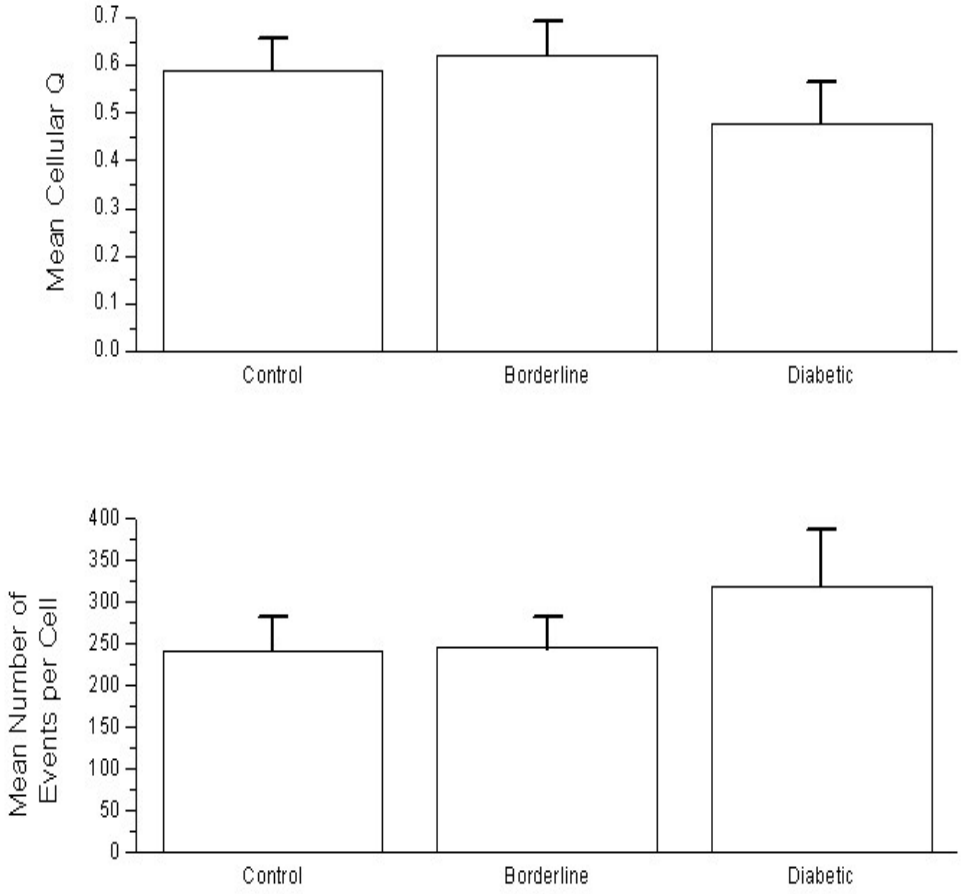

The mean cellular quantal size (A) and the mean number of events per cell (B) from a control, borderline diabetic and diabetic Nile rat. N=15 cells for the control and diabetic chromaffin cells and N=13 for the chromaffin cells from the borderline diabetic Nile rats.

Figure II:

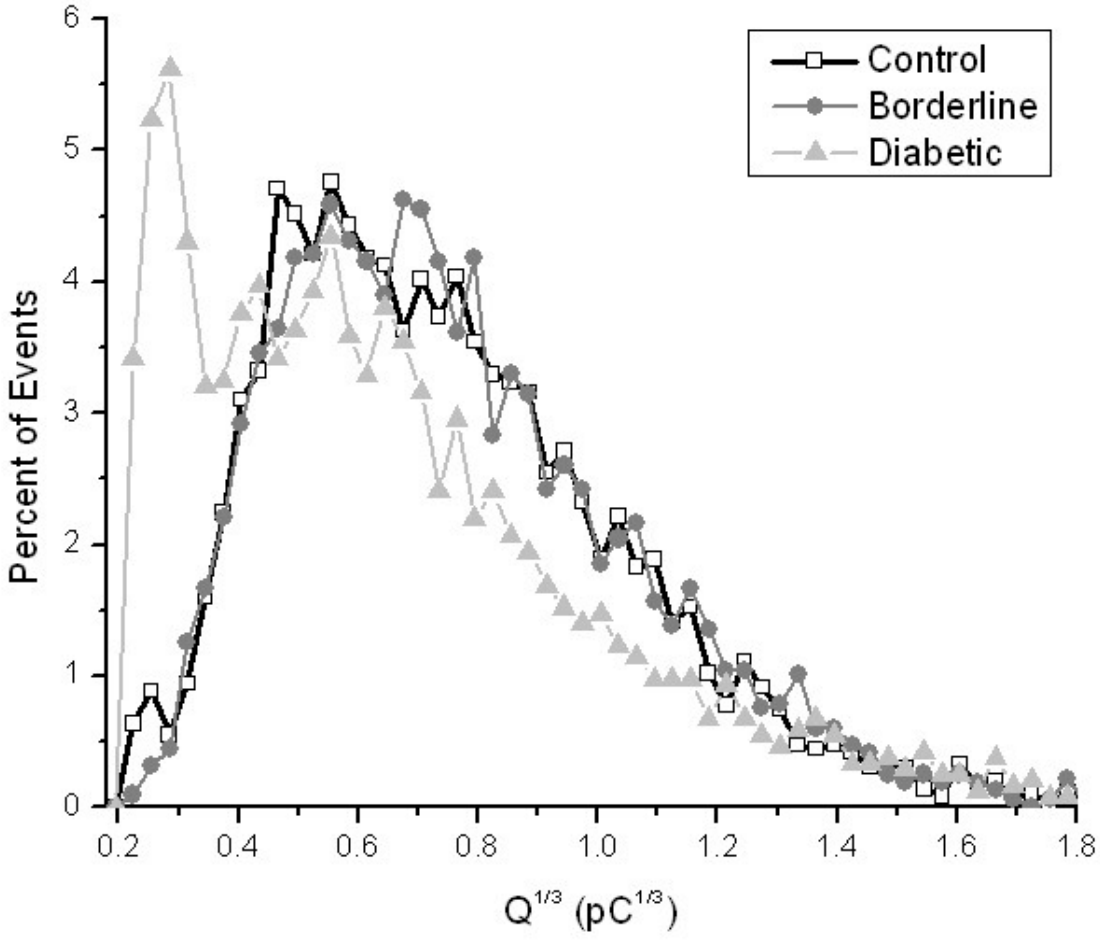

The distribution of events with the cube root of Q for control cells and cells from fructose-fed rats. N= 3615 events for the control cells, 2376 events for the cells from the diabetic Nile rat and 3186 events for the cells from the border line diabetic Nile rat. A Kolmolgrov-Smirnov test on the cumulative distribution of the control and the borderline diabetic had a $p > 0.05$ which means these two distributions are not significantly different. A Kolmolgrov-Smirnov test on the cumulative distribution of the control and the diabetic had a $p < 10^{-4}$, which means these two distributions are significantly different.

Figure III:

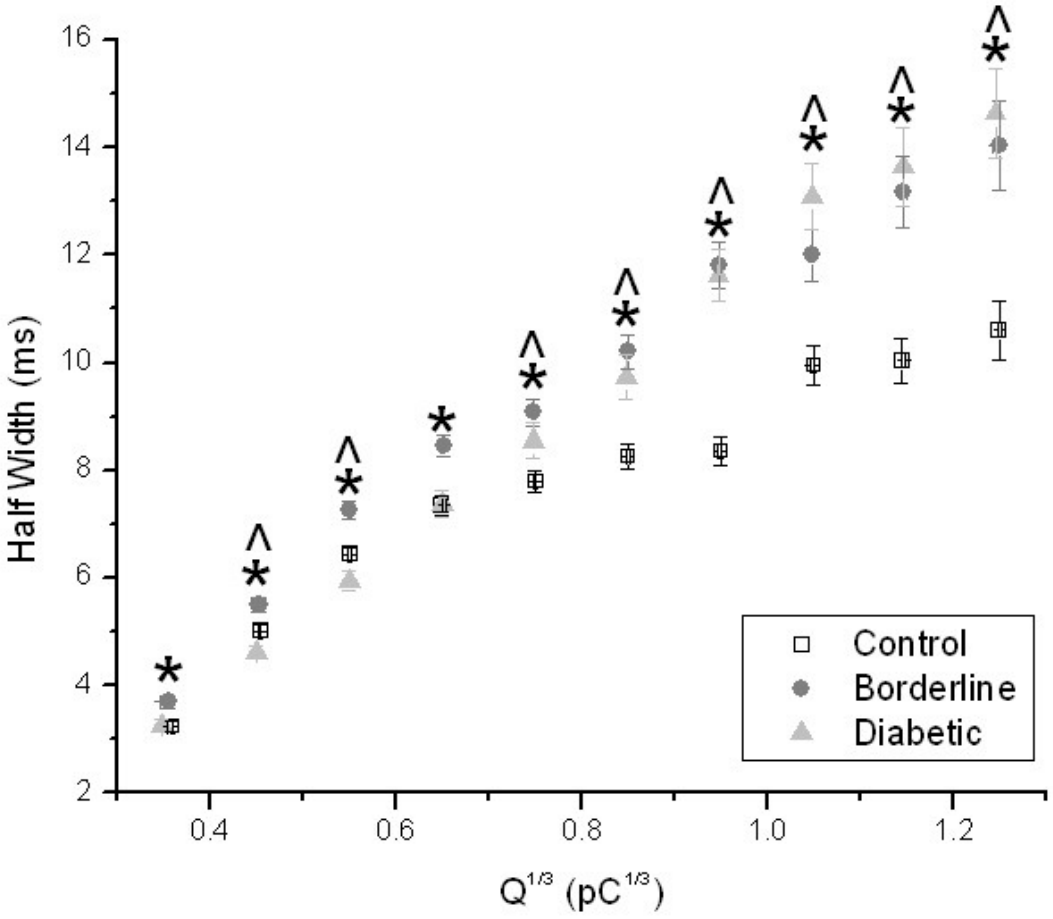

The spike half width at matched bin size of 0.1 $pC^{1/3}$. * indicates $p<0.05$ between the control and borderline group and ^ indicates $p<0.05$ between the control and diabetic group. N= 3615 events for the control cells, 2376 events for the cells from the diabetic Nile rat and 3186 events for the cells from the border line diabetic Nile rat

Figure IV:

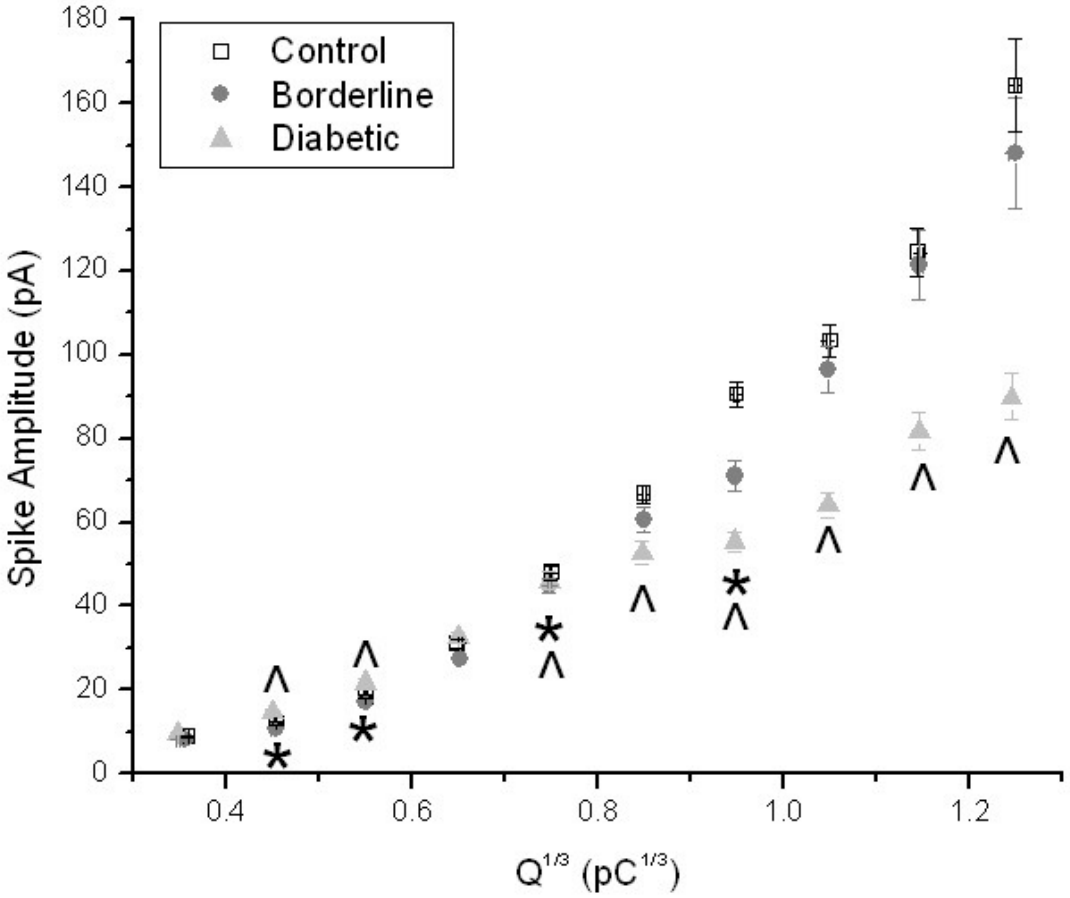

The spike amplitude at matched bin size of 0.1 $pC^{1/3}$. * indicates $p<0.05$ between the control and borderline group and ^ indicates $p<0.05$ between the control and diabetic group. N= 3615 events for the control cells, 2376 events for the cells from the diabetic Nile rat and 3186 events for the cells from the border line diabetic Nile rat

Reference List:

Noda K, Melhorn MI, Zandi S, Frimmel S, Tayyari F, Hisatomi T, Almulki L, Pronczuk A, Hayes KC and Hafezi-Moghadam A (2010). *The FASEB Journal.* **24:** 2443-2453.